

NSF/CEE-82002

FB82-246794

THE SHARPSBURG, KENTUCKY EARTHQUAKE
OF JULY 27, 1980

FORWARD

The Sharpsburg, Kentucky earthquake of July 27, 1980, with a m_{bLg} magnitude of $5\frac{1}{4}$ and a M_S magnitude of 4.9, was generated by a predominately right-lateral strike-slip motion orientated in a $N30^\circ E$ direction, and caused damages on the order of \$4,000,000. The earthquake is an important event in the effort of quantify eastern North American (i.e., that area east of the Rocky Mountains) seismicity because it took place in an area where most researchers did not expect an earthquake of such magnitude, and because the quantity and quality of the noninstrumental and instrumental data is such that this earthquake is by far the most thoroughly studied and documented earthquake to date, in eastern North America.

This report consists of two sections. The first section contains a detailed report on the effects of the earthquake within the $3,600 \text{ km}^2$ designated meizoseismal area. The second section discusses the surface-wave, P-wave first motion, and teleseismic data used to derive a focal mechanism, as well as a discussion on the detailed aftershock study which most importantly identified the $N30^\circ E$ striking nodal plane of the derived focal mechanism as the rupture plane of the main shock.

Any opinions, findings, conclusions or recommendations expressed in this publication are those of the author(s) and do not necessarily reflect the views of the National Science Foundation.

TABLE OF CONTENTS

Page

THE SHARPSBURG, KENTUCKY EARTHQUAKE OF JULY 27, 1980

FORWARD

ARCHITECTURAL AND STRUCTURAL DAMAGE, AND GROUND EFFECTS
 RESULTING FROM THE JULY 27, 1980 SHARPSBURG, KY
 EARTHQUAKE

ABSTRACT.	1
INTRODUCTION.	2
MAXIMUM INTENSITY	3
MM INTENSITY SURVEY OF THE MEIZOSEISMAL AREA.	4
Minor Architectural Damage	5
Chimney Damage	5
Brick Walls and Veneer	7
Cracks In Basement Walls	8
Damage Due to Weak Structural or Geological Foundation Conditions	9
Damage to Well Constructed Structures.	11
Tombstones	14
Ground Effects	14
Highway Bridges.	16
Misleading or Incorrect Reports of Earthquake Related Damage	17
MONETARY COST OF DAMAGES.	18
SUMMARY	20
ACKNOWLEDGMENTS	22
APPENDIX A: Damage Sustained in Maysville, KY as a Result of the July 27, 1980 Earthquake	54

INSTRUMENTAL STUDIES OF THE SHARPSBURG, KENTUCKY EARTHQUAKE
 OF JULY 28, 1980

ABSTRACT.	60
INTRODUCTION.	62
MAIN SHOCK SOURCE STUDIES	62
Surface Wave Studies	62
Regional Waveform Studies.	64
Body Waveform Studies.	66
AFTERSHOCK STUDIES.	69
Data Analysis.	72
Discussion	74
CONCLUSIONS	77
ACKNOWLEDGMENTS	77
REFERENCES.	79

ARCHITECTURAL AND STRUCTURAL DAMAGE,
AND GROUND EFFECTS RESULTING FROM
THE JULY 27, 1980 SHARPSBURG, KY
EARTHQUAKE

By

R. Street and W. Foley

Dept. of Geology
University of Kentucky
Lexington, KY 40506

ABSTRACT

The 5.3 m_bLg magnitude earthquake that occurred near Sharpsburg, KY on July 27, 1980, caused in excess of three million dollars worth of damage within a 3,600 km² meizoseismal area. Based on a number of criteria, including damaged chimneys, cracked exterior and basement walls, rotated and displaced tombstones, and miscellaneous ground effects, the meizoseismal area is judged to represent the intensity VI (MM) area of the earthquake. And within the meizoseismal area, the towns of Sharpsburg and Maysville, KY are judged to have experienced a sufficient number of effects to have been assigned an intensity VII (MM).

Introduction

The Modified Mercalli (MM) intensity VII earthquake of July 27, 1980 caused in excess of three million dollars worth of damage to homes, businesses, schools, churches, and a state park within a 3,600 km² sparsely populated area of north-central Kentucky. The area bounded by Paris, KY to the west, Owingsville, KY to the east, Mt. Sterling, KY to the south, and Ripley, OH to the north is designated in this paper as the meizoseismal area of the event, and is outlined in Figure 1 by the dashed lines. Not incorporated in the meizoseismal area are the isolated, but numerous instances of broken chimneys, cracked basement walls, ground cracking, changes in well water levels, and cracked or dislodged parapet damage reported throughout central Kentucky.

For the most part, damage to structures within the meizoseismal area was of the architectural variety, however several instances of damage involving the structural integrity of buildings were also documented. In addition, ground effects, such as landslides, changes in well and pond water levels, and soil cracking occurred throughout the southern portion of the meizoseismal area - effects that are explained by specific soil and foundation conditions rather than severe ground-motions.

The purpose of this paper is to report on an extensive set of first-hand field observations regarding the structural and ground phenomena attributed to the Sharpsburg, KY earthquake. Data from questionnaires distributed in the meizoseismal area, and from requests for information published in

regional newspapers were used as a guide to follow-up field studies that continued for several months after the occurrence of the event.

Maximum Intensity

Two localities, Sharpsburg and Maysville, KY, experienced a sufficient number of Modified Mercalli (MM) intensity VII effects to be characterized as sites of MM intensity VII. In the rural area immediately about Sharpsburg, a village with a population of 400, a few homes were shifted on their foundations, 35% of the chimneys were damaged, four well built homes were severely damaged, portions of the brick veneer on four additional homes were knocked off, individuals in two homes as well as mourners attending a funeral in the village cemetery reported difficulty in standing, and reports of three small landslides, muddied water and changes in well water levels, and three instances of the earthquake being felt in moving vehicles were received. In addition, there were numerous other reports of minor cracking in foundations, water wells, cisterns, plastering, brick veneer, driveways, and outdoor patios.

The MM intensity assigned to Maysville, a town with a population of 7,000, is based on two instances of slope failure, the widespread chimney damage, and the cracked brick walls and chimneys as well as the fallen parapets and ornaments within the twelve square block area bounded by Fifth Street,

McDonald Parkway, Sutton Street, and Clarks Alley in the central part of town. A more detailed description of the damage in Maysville is given in Appendix A.

The criteria used to assign the MM intensity VII at the two localities is, therefore, somewhat different. In Sharpsburg, the MM intensity VII is assigned on the basis of the ground effects and damage done to one and two story homes of both older and newer construction; while in Maysville, the MM intensity VII is based on damage done to multistory older homes, and older commercial and public buildings. The usage of different criteria is a result of (1) the population difference, and (2) the fact that nearly all of the damaged commercial and public buildings in Maysville are older multistory structures, whereas the few commercial structures in Sharpsburg are generally single story and significantly newer than those damaged in Maysville.

MM Intensity Survey of the Meizoseismal Area

In the following paragraphs, a summary of the MM intensity effects documented within the meizoseismal area of the July 27, 1980 Sharpsburg, KY earthquake are given. Within the rural countryside and small farming communities that make up the meizoseismal area, a sufficient number of MM intensity VI or greater effects were observed, that we consider the area as a whole as constituting the MM intensity VI area.

Minor Architectural Damage

There were numerous and widespread instances of minor architectural damage, such as broken glass, cracked or fallen plaster, and damage to decorative brickwork, reported throughout the meizoseismal area. Figures 2 and 3 illustrate examples of this type of damage in Maysville, Kentucky; Figure 2 shows a broken 1/2 inch plate glass bank window, while Figure 3 is of a brickfall from a damaged parapet. Figure 4 shows a window in the courthouse at Flemingsburg, Kentucky from which the cornice was shaken loose, while Figure 5 shows the cracked cornice on the two-story Perfect Lady Beauty Shop in Owingsville, Kentucky.

Scattered instances of minor architectural damage were also reported well outside of the meizoseismal area. The furthest such report received, was from Pine Knot, Kentucky that is 175 kilometers to the south of the epicenter. At the home of Mrs. Mabel Tartar on Rt. 1, several small cracks were found between the brickwork near the front wall of the house, with one large crack beginning at the foundation to a point halfway up the front wall of the house. Other minor architectural damage reports were received from Cincinnati, Ohio to the north, and Prestonburg, Kentucky to the east.

Chimney Damage

The most prevalent and obvious type of damage to occur in the meizoseismal area was chimney damage, which ranged from a few bricks being dislodged at chimney tops, to instances of chimney falls and chimneys being broken near the roofline.

Figures 6 thru 12 illustrate the range of chimney damage sustained. In Figure 12, approximately three feet of the chimney was broken off. Bricks from the chimney were scattered about the yard with some being found as far as fifteen feet away from the side of the house.

Factors that contributed to the extensive chimney damage were (1) the age and type of mortar used between the chimney brickwork, and (2) the lack of chimney flues in many of the older homes. Homes with chimney damage were generally built before World War II, with many dating back to the turn of the century. Mortar used between the bricks of the chimneys of the older homes consists of a locally produced limestone based mortar that is susceptible to weathering. Figure 13 shows dislodged bricks from the damaged chimneys on the two story wood-frame Hall residence in Mt. Sterling, KY. Severe weathering of the mortar used in the construction of the chimney is indicated by the deep grooves between the bricks, and by the lack of mortar on the brick faces of the dislodged bricks; mortar shows up in the figure as white patches on the brick faces.

Another factor that contributed to the extensive chimney damage in the meizoseismal area, is the nearly uniform lack of chimney flues in the construction of the older homes. Not only were the chimneys without flues subject to greater damage above the roofline than those with flues, but many such chimneys were cracked well below the rooflines and became potential fire hazards.

Based on conversations with brick masons and homeowners,

the cost of repairing a chimney ranged from a low of \$80 for minor repairs involving chimney tops, to \$500 for those repairs to chimneys cracked below the roofline. The latter type of damage was generally repaired by inserting a linear into the chimney and filling the void between the linear and chimney with cement.

Brick Walls and Veneer

Numerous examples of brick walls being cracked along mortar joints were observed and reported throughout the meizoseismal area. Figures 14, 15 and 16 illustrate three such instances of cracking. Figures 14 and 15 are of buildings in Aberdeen, Ohio and Lewisburg, Kentucky respectively, which are towns, in the northern extremity of the meizoseismal area. At the southern edge of the meizoseismal area, Figure 16 shows a similar type of cracking in a concrete block structure on the Mt. Sterling Golf Course.

Figures 17 and 18 illustrate still another type of damage to brick walls that was experienced in the epicentral region about Sharpsburg, KY. Figures 17 and 18 show the damage to the brick veneer of the back and front walls of the two-year old wood-frame Golden residence that is located approximately 10 kilometers west of Sharpsburg. Brick veneer on the back wall of the house was shaken off from the roofline down to the level indicated by the arrow in Figure 17, while the brick veneer on the front of the house was pulled out from the wall and would have collapsed, except for the support of the molding about the window frame as shown in Figure 18.

Three other homes in the epicentral area had their brick veneer severely damaged by the ground-motions of the earthquake. One home was the new Vice residence on Kentucky Rt. 32, 3 kilometers from Carlisle, Kentucky, another home was a 10 year old Bedford style house in Sharpsburg, while a third house was a newer home in Little Rock, Kentucky. Damage to the brickwork on the Vice house was \$4,500 while that to the other homes were on the order of a couple of thousand dollars.

In addition to brick veneer being shaken off homes, numerous other homes owners in the meizoseismal region reported cracking in the mortar between the brickwork.

Cracks in Basement Walls

Several instances of severe damage to cisterns and basement walls in the southern and central portions of the meizo-seismal area were reported. Figure 19 shows the basement wall at the Cooper's residence in Flemingsburg, KY that was both cracked and bowed by the ground-motions of the earthquake. Figure 20, also from the Flemingsburg area, shows the cracked boiler room stairwell in the basement of the Fleming County Hospital. Severely cracked basement walls were also observed in the North Middletown, Sherburne, Owingsville, Sharpsburg, and Little Rock, KY localities.

Besides the severe damage to the cisterns and basement walls at the localities listed above, widespread reports of minor cracking in cisterns and basement walls were received from Carter, Elliott, Fleming, Rowan, Bath, Montgomery, Mason, Bourbon, Nicholas, Clark, and Fayette counties in north-central

Kentucky, as well as one such report each from Wayne and McCreary counties in southeastern Kentucky.

Damage Due to Weak Structural or Geological Foundation Conditions

Some of the more severely damaged structures resulting from the Sharpsburg earthquake, were those with poorly designed or weakened structural foundations. An example of a structure that sustained severe damage due in part to a poorly designed structural foundation, is the 40 x 100 foot two story concrete block Morning Star Baptist Church in Owingsville, KY. The structure had been built in the early 1960's on the side of a steep hill with a footing that was not properly secure to the bedrock. During the earthquake, the rear quarter of the structure separated from the remainder of the building, and slide down the hillside 2 inches before stabilizing. Figure 21 shows the separation in the south wall of the exterior of the building, while Figure 22 shows the twisted pillars in the interior of the church basement. As a result of the earthquake, the Morning Star Baptist church building was condemned, torn down, and replaced by a new structure.

Figure 23 is a picture of a badly damaged 150 year old Purvis residence one kilometer south of Sharpsburg. The damage to the Purvis house is an example of a building that sustained severe damage primarily as a result of a structural foundation that had been seriously weakened by age and weathering. The cracks about the door frames in the figure are typical of the cracking that occurred throughout the exterior and interior walls of the house. Some of the cracks were large enough

that one could see, without difficulty, into the interior of the house from the outside. As with the Owingsville Morning Star Baptist Church, the Purvis house has been condemned by the local building inspector, and has since been abandoned.

As a point of interest, the reason the windows in the Purvis house shown in Figure 23 were not broken, is that they were of Plexiglass instead of glass.

An example of extensive damage being due in part to unfavorable ground conditions, is the damage at Blue Licks State Park that is west of Mt. Olivet, KY. Figures 24, 25, and 26 illustrate just a few examples of the extensive cracking of the bathhouse, pool deck area, and a picnic shelter at the park. In addition to these facilities, the park superintendent's house and park museum which are substantial fieldstone structures, as well as the walls of the pool were extensively cracked. In the case of the pool deck area, pool, and bathhouse, a likely explanation for the damage is the fact that these facilities were built ten years ago on a man-made fill that probably underwent further compaction as a result of the earthquake. The cause of the cracking and differential settling of the concrete floor in the picnic shelter in Figure 26, as well as the other picnic shelters in the park, the museum, and the park superintendent's house, is not as obvious. These structures were all built on natural terrain which, in particular, seems to preclude a differential settling on the order of the 1 inch that was observed at the picnic shelter shown in Figure 26.

Damage to Well Constructed Structures

There were a few instances of severe damage being sustained by apparently well built structures that were (1) in a good state of repair, (2) had a substantial foundation, and (3) were situated on natural terrain. Figure 27 shows the interior view of the living room fireplace in the Carpenter residence on the Bunker Hill road approximately 3 kilometers west of Judy, Kentucky. In addition to the fireplace mantle being pulled away from the wall, the house sustained cracked and buckled walls both upstairs and downstairs, damage to a chimney, dislodged bricks from another fireplace, and a cracked foundation. The home is a 100 year old recently remodeled two story wood-frame house that appears to have been carefully maintained. Damage to the house was substantial, with the plaster damage alone costing \$3,500.

Another home that suffered extensive interior damage was the two-story Clay residence on Flat Creek road 2 kilometers east of Sharpsburg. The house consists of two parts, an older masonry section dating back about 70 years and a small wood-frame section of approximately 10 years in age. Structural damage to the house was restricted to the older section, although the newer section was severely shaken as demonstrated by the articles thrown off shelves, opened cupboard doors with contents on floor, and a broken chandelier. Figure 28 shows a typical corner between the front of the house and a second floor interior partition. Even more dramatic was the movement of the ceiling on the second floor of the older section of the

house with respect to the interior partitions. On the southwest side of the house, the second floor ceiling was displaced nearly 2 inches with respect to the interior walls. Unfortunately, pictures showing this movement were inadvertently destroyed during the developing process.

The Toy residence, about 5 kilometers southeast of Sharpsburg on the Bennett Branch road, also suffered extensive damage from the earthquake. Figure 29 shows the west side of the house that was buckled inwards; the east side wall was buckled outwards. Figure 30 shows the cracked concrete blocks in the well house that sets on naturally level terrain on the east side of the house. Figure 31 shows the severed water pipe that went from the well house through the basement wall to the hotwater heater that was overturned during the earthquake. Figure 32 shows one side of the two-story concrete block garage on the Toy farm. And, as in the case with the concrete block well house, the crack passes through the concrete blocks, not just along the mortar joints. Unlike the house and well house though, the garage was built into the side of a hill with a gentle slope off to the right of the wall shown in Figure 32. The motion inside of the house, as a result of the earthquake, is described by Mr. Toy as being ". . . so bad that I and my family found it difficult to stand".

Four kilometers east of Sharpsburg on Flat Creek road, the hundred year old two-story brick home of Mr. Raymond Stull was extensively damaged by the earthquake. The cemented limestone foundation on the west side of the house was bowed

outwards 7 to 8 inches, the three chimneys on the house were damaged - with the chimney on the west side of the house being split from the roofline to the fireplace, while the screws holding the mantle to the wall over the fireplace on the east side of the house were pulled out of the wall about 2 inches. Damage to the house also included a room on the first floor of the east end of the house that was noticeably twisted out of alignment with the rest of the house; the wallpaper in this room was torn in a manner suggesting a twisting or shear-type of motion. In addition, cupboards were emptied of their contents, pictures were knocked off walls, and Mrs. Stull and her daughter, who were in the house during the earthquake, reported that they were unable to stand during the event. Figures 33 and 34 illustrate a portion of the damaged limestone foundation along the front of the Stull residence, and crumpled and torn wallpaper in the corner of the first floor room at the east of the house.

Another structure that was severely damaged by the earthquake, was the Mt. Sterling Middle School on Kentucky Rt. 11 in Mt. Sterling, KY. The three-story brick building was completed in the early 1930's and appears to have been kept in a good state of repair. Figure 35 shows the third floor of the south wall which was so badly damaged that one window was removed and bricked over, and the lintel over the window to the right was knocked out about 2 inches from the wall. This section of the exterior wall required \$22,000 dollars in repairs immediately after the main shock, in order to stabilize the

wall from further movement. Figure 36 is an interior shot of the typical type of damage done to the window pillars on the south side of the second floor of the building, while Figure 37 shows the type of interior damage typically found along the north wall of the building. Total damages to the structure was estimated by the city's architect to be on the order of \$325,000.

Tombstones

Tombstones throughout the meizoseismal area were effected by the ground-motion of the earthquake. Based on our observations, the movement of the tombstones was random; that is, we observed tombstones - in the same cemetery - that had rotated clockwise, counterclockwise or shifted on their pedestal with somewhat equal regularity. Figures 38, 39 and 40 illustrate three tombstones in the Sharpsburg valley cemetery that give evidence of rotation, displacement, and partial overturning, respectively. A few tombstones in the cemetery were completely overturned by the earthquake, but were righted by the ground-keeper the day after the event.

Ground motions at the Sharpsburg village cemetery not only effected tombstones, but were also noticeable to mourners attending a funeral. They described the ground-motion as severe enough to make it difficult to stand, and to be noticeable in slowing moving cars.

Ground Effects

The Sharpsburg earthquake caused ground cracks, landslides,

and changes in well water. Figure 41 illustrates the geographical distribution of the reported ground cracking, while Figure 42 is a closeup of a ground crack in Owingsville, Kentucky that is typical of those reported. The Owingsville ground cracking occurred extensively throughout an open field on a hillside of 8° slope that is covered with 4 to 6 feet of soil of high clay content. The ground cracking at the Lexington, Hillsboro, and Morehead sites indicated in Figure 41 occurred under similar circumstances; i.e., on open slopes covered with soil high in clay content. These conditions, plus the fact that central Kentucky experienced a severe drought during the summer of 1980, leads us to the conclusion that the cracks are essentially dessication cracks triggered by the earthquake.

Another ground effect attributed to the Sharpsburg earthquake, were the three instances of landslides in the epicentral region as indicated in Figure 41. Figure 43 shows one such landslide in a road cut near the junction of Hinkston Creek, and the boundary of Nicholas and Bourbon counties - approximately seven kilometers west of Sharpsburg. The rock matrix in this area consists of alternating layers of weak shales and limestones that are very susceptible to weathering. Consequently, the landslides are considered to be a secondary effect triggered by the earthquake, and not necessarily indicative of appreciable ground-motions.

The third type of ground effect reported as a result of the Sharpsburg earthquake was changes in well water. Figure 44 illustrates the distribution of the changes in the well

water that were documented during the course of this study. In the figure, (M) indicates a report of muddied well water, (+) indicates an increase in the well water level, and (-) indicates a decrease in the well water level. The decreases in the water levels shown in the lower right-hand corner of the figure are the most reliably documented, since the water level in the well and adjacent natural pond were being used in a water monitoring project. The water level in the well dropped eight feet while the water level in the pond dropped about two feet shortly after the occurrence of the earthquake. These changes in the water level, as with those changes in the water levels documented elsewhere, appear to be permanent. In addition to the changes in the water levels shown in Figure 44, reports by county agricultural agents and conversations with farmers in Clark, Montgomery, Robertson, and Bath counties suggests that the changes in water levels were probably substantially more widespread than those which we were able to document.

Highway Bridges

As part of the field investigation of the earthquake, a visual inspection of the highway bridges in the region about the epicenter was conducted to determine whether any of the bridges showed signs of having moved as a result of the event. This inspection consisted of a check of joints such as those found between bridge spans and their support columns. Of the bridges inspected, the only one that apparently moved during the event was a sixty foot, simple truss bridge built

in 1892 on the Nicholas and Bath county line eight kilometers west of Sharpsburg.

The freshly painted, broken tie-rod that supports the wooden railing shown in Figure 45, is typical of the damage done to the tie-rods on the northern and southern corner of the northeast-southwest orientated bridge. Tie-rods for the wooden railings on the opposite two corners were not noticeably effected. While the upper portion of the bridge was apparently twisted during the earthquake, an inspection of the paint on the rollers and tie-rods between the ends of the bridge span and bridge abutments, indicated that the bridge as a whole did not move.

Misleading or Incorrect Reports of Earthquake Related Damage

During the course of documenting the effects of the Sharpsburg earthquake, a few instances of seemingly significant damage were found to be incorrect. In Owingsville, KY it was widely reported that the ceiling of the Catholic church on Main Street had suffered extensive damage as a result of the quake. This report was seemingly substantiated by the fact that the church was closed immediately after the earthquake and all persons were barred from entry. However while trying to obtain an estimate as to the cost of damages sustained by the church, the office of the local diocese informed us that the ceiling of the church was in a badly deteriorated state of repair due to a leaking roof prior to the earthquake, and that in their opinion the earthquake had merely aggravated an existing problem and advanced the schedule of the necessary repairs.

Another example of seemingly significant earthquake related damage that is misleading, is the cracked concrete block wall of the Calvery Baptist Church in Maysville, KY shown in Figure 46. The cracking observed in the church wall near the roofline follows along a pre-existing crack that had been previously patched and stabilized by tie-rods. Also in Maysville, an example of damage being incorrectly attributed to the earthquake, is the report of an underground water main being broken on Fourth Street. A check with the Maysville Department of Water Resources indicates that the water main had been leaking, and was dug up prior to the occurrence of the earthquake.

Monetary Cost of Damages

As stated in the introduction, the July 27, 1980 earthquake resulted in excess of three million dollars worth of damages to homes, businesses, schools, churches, and a state park within an area we have designated as the meizoseismal area. Table 1 is a breakdown of the estimated cost of damages by county, and type of structure. The damage figures are based on information compiled by the Small Business Administration(SBA), Diaster and Emergency Services (ES), the Park Superintendent at Blue Licks State Park, and our conversations with homeowners and brickmasons. Under the category of damage to residences, we include chimney damage as well as the more severe damage such as that previously described at the

Stull residence. Not included in the estimated cost of damages, are the costs for repairing the many basement walls cracked during the earthquake. A local company that specializes in waterproofing basements, estimates that damage per basement range upward to a few thousands of dollars, depending on the extent of resealing that was necessary.

The accuracy of the monetary damages listed in Table 1 needs to be qualified. The most accurate estimate of damages are probably those given for Mason County since the damages in that county were concentrated in the city of Maysville which received widespread publicity at the time of the event. The most inaccurate cost of damages given in Table 1, are probably those listed for Bath, Fleming, and Montgomery counties. Damages in these counties were primarily in rural areas, received little publicity, and consequently were very difficult to document.

In summary, with respect to Table 1, we have documented three million dollars worth of damage within the meizoseismal area as a result of the July 27, 1980 earthquake. It is our conclusion, however, that a more accurate monetary cost of damages is probably on the order of four million dollars if basement damage, damage outside of the meizoseismal area, and the probably underestimated damage figures in Bath, Fleming and Montgomery counties are taken into consideration.

Summary

This report presents the observations and information gathered during a year long follow-up study in the meizoseismal area of the July 27, 1980 Sharpsburg, KY earthquake. Important results of this study are as follows:

1. Maximum Modified Mercalli (MM) intensities of VII were experienced in the area of Sharpsburg and Maysville, KY;
2. the remainder of the 3,600 km² meizoseismal area generally experienced MM intensity VI or greater effects; and
3. the estimated monetary value of the damage attributed to the Sharpsburg earthquake was on the order of four million dollars.

Not included in this paper, are the results from the follow-up of the numerous miscellaneous reports of minor damage outside of what we have designated as the meizoseismal area. We know, for example, of ten chimneys being damaged and several instances of plaster and basement walls being cracked in the Lexington, KY area, of at least eight chimneys being damaged in northeastern Jessamine county, and that the home of Mr. Fred Barnsdale near Elliottville, KY was shifted by a quarter of an inch on its cement block foundation. In addition to these reported instances of damage, we suspect that there were several other unreported instances of minor damage.

outside of the meizoseismal area, particularly in the sparsely populated region to the south and southeast of the meizoseismal boundary shown in Figure 1.

ACKNOWLEDGMENTS

The detailed intensity survey described in this study, and the extensive aftershock study and monitoring program described in the joining paper by Herrmann et al., would not have been possible without the enthusiastic help and long hours of effort by Mr. James Zollweg of Tennessee Earthquake Information Center and the following University of Kentucky students: Mark Allsop, Kevin Brumfield, Mike Netzband, Chris Steinemann, Patricia Wonderley and Wendy Wonderley.

We also acknowledge and sincerely appreciate the allocation of funds arranged for us by Mr. Clifford Swager of the University of Kentucky and Dr. Andrew Murphy of the Nuclear Regulatory Commission, without which the costly field studies could not have been completed.

This research was supported in part by the U.S. National Science Foundation under grant No. PFR-7819765. The opinions, findings and conclusions or recommendations expressed in this manuscript are those of the authors, and do not necessarily reflect the views of the National Science Foundation.

TABLE CAPTION

Table 1. Estimated cost of damages within the meizoseismal area of the July 27, 1980 Sharpsburg, Kentucky earthquake.

FIGURE CAPTIONS

- Figure 1. Meizoseismal area of the July 27, 1981 Sharpsburg, KY earthquake. Epicenter, at Sharpsburg, is represented by open triangle.
- Figure 2. One-half inch broken plate glass bank window at street level in downtown Maysville. Photo by courtesy of J. Parker.
- Figure 3. Brick fall from broken parapet in downtown Maysville, KY. Photo by courtesy of J. Parker.
- Figure 4. Window cornice shaken loose from courthouse, in Flemingsburg, KY.
- Figure 5. Cracked cornice on second story of Perfect Lady Beauty Shop in Owingsville, KY.
- Figure 6. Chimney damage at Robert's residence in Sharpsburg, KY.
- Figure 7. Broken chimney at the top of the west wall of the two story Toy residence near Sharpsburg, KY.
- Figure 8. Typical chimney damage in downtown Maysville. Photo by courtesy of J. Parker.
- Figure 9. Chimney damage at abandoned residence on Route 11 south of Moorefield, KY.
- Figure 10. Chimney damage at 152 Main Street, Owingsville, KY.
- Figure 11. Chimney fall at one story frame structure at Sherburn, KY. Notice that the chimney has no flue for internal support, and that the mortar is in poor condition.
- Figure 12. Chimney damage at Brewer residence on Route 11 north of Sharpsburg. Notice the condition of the mortar.
- Figure 13. Chimney damage at two story frame Hall residence in Mt. Sterling. Notice poor condition of mortar.
- Figure 14. Cracked brick wall in school one block from Ohio River in Aberdeen, OH.
- Figure 15. Cracked brick wall in six year old residence in Lewisburg, KY (see arrow).
- Figure 16. Cracks in concrete block structure at golf course in Mt. Sterling, KY. Photo by courtesy of J. Zollweg.

- Figure 17. View of the rear of the Golden residence where brick veneer was shaken off down to the level indicated by the arrow. The structure is approximately 10 kilometers west of Sharpsburg, KY, and is two years old.
- Figure 18. Same structure as shown in Figure 17, but view shows the front of the house where the brick veneer is pulled out from around the window frame (see arrow).
- Figure 19. Cracked and bowed concrete block basement wall at Cooper residence in Flemingsburg, KY.
- Figure 20. Cracked stairwell in the boiler room of the Fleming County Hospital in Flemingsburg, KY.
- Figure 21. Cracked and separated exterior wall of the Morning Star Baptist Church in Owingsville, KY.
- Figure 22. Displaced near pillar in the basement of the Morning Star Baptist Church in Owingsville, KY (see arrow).
- Figure 23. Extensive cracking in the 150 year old brick Purvis home on the outskirts of Sharpsburg, KY.
- Figure 24. Cracked foundation in the poolhouse at Blue Lick State Park, KY.
- Figure 25. Cracked cement pool deck, believed to be caused by settling of manmade fill, at Blue Lick State Park, KY.
- Figure 26. Cracked cement floor of a picnic shelter at Blue Lick State Park, KY.
- Figure 27. Separation of fireplace mantle from wall at the Carpenter residence near Judy, KY. Photo by courtesy of TVA.
- Figure 28. Plaster crack in second story bedroom of the Clay residence near Sharpsburg, KY.
- Figure 29. View of the west wall of the Toy structure near Sharpsburg, KY. Notice how the wall is bowed inwards (see arrow); east wall of the structure was bowed outwards in a like manner.
- Figure 30. Cracked cement block well house on the Toy farm near Sharpsburg, KY.
- Figure 31. Broken 1 inch water pipe in cellar of well house on the Toy farm near Sharpsburg, KY. Broken water pipe was attached to a free standing four foot tall by two foot diameter water tank that was knocked over by the earthquake.

- Figure 32. Crack in concrete block sidewall of the two story garage on the Toy farm near Sharpsburg, KY. The structure is built on the west slope of a hill, and the rear wall of the structure was shifted down slope.
- Figure 33. Workman repairing the damaged limestone foundation of the Stull residence near Sharpsburg, KY. This section of the foundation was badly cracked, and displaced by as much as eight inches as result of the earthquake. Photo by courtesy of Mrs. R. Stull.
- Figure 34. View of the torn wallpaper along the corner of the first floor east end room of the Stull home near Sharpsburg, KY. Photo by courtesy of Mrs. R. Stull.
- Figure 35. Damaged exterior south wall of the middle school in Mt. Sterling, KY. One window was removed and bricked in, as was the stone lintel over the window to the right (see arrows).
- Figure 36. Damaged to one of several window pillars on the second floor of the middle school in Mt. Sterling, KY.
- Figure 37. Typical damage to the interior of the north wall on the second floor of the middle school in Mt. Sterling, KY.
- Figure 38. Clockwise rotation of stone monument in the Sharpsburg cemetery - penny for scale.
- Figure 39. Example of stone monument in the Sharpsburg cemetery that was shifted approximately $\frac{3}{4}$ of an inch.
- Figure 40. Example of a tombstone in the Sharpsburg cemetery that would have fallen if not for the metal rods connecting the top to the base.
- Figure 41. Map illustrating the distribution of some of the ground cracking (X) and landslides (L) reportedly resulting from the earthquake.
- Figure 42. Ground cracking in Owingsville, KY that is believed to be desiccation cracks triggered by the earthquake. Pen for scale.
- Figure 43. Small rockslide in roadcut near the Nicholas Co.-Bourbon Co. line that was triggered by the earthquake.
- Figure 44. Map illustrating the changes in well water levels (+ for increase flow; - for decrease flow), and muddied water (M) as a result of the earthquake.
- Figure 45. View of a broken and twisted tie-in rod observed on a small bridge on the Nicholas Co.-Bourbon Co. line (see arrow; half dollar is used for scale).

Figure 46. Previously cracked concrete block wall in the Calvary Baptist Church in Maysville, KY that was reopened by the earthquake. Photo by courtesy of TVA.

JULY 27, 1980
18:52:23 (GMT)
38.2° N / 83.9° W

MEIZOSEISMAL AREA

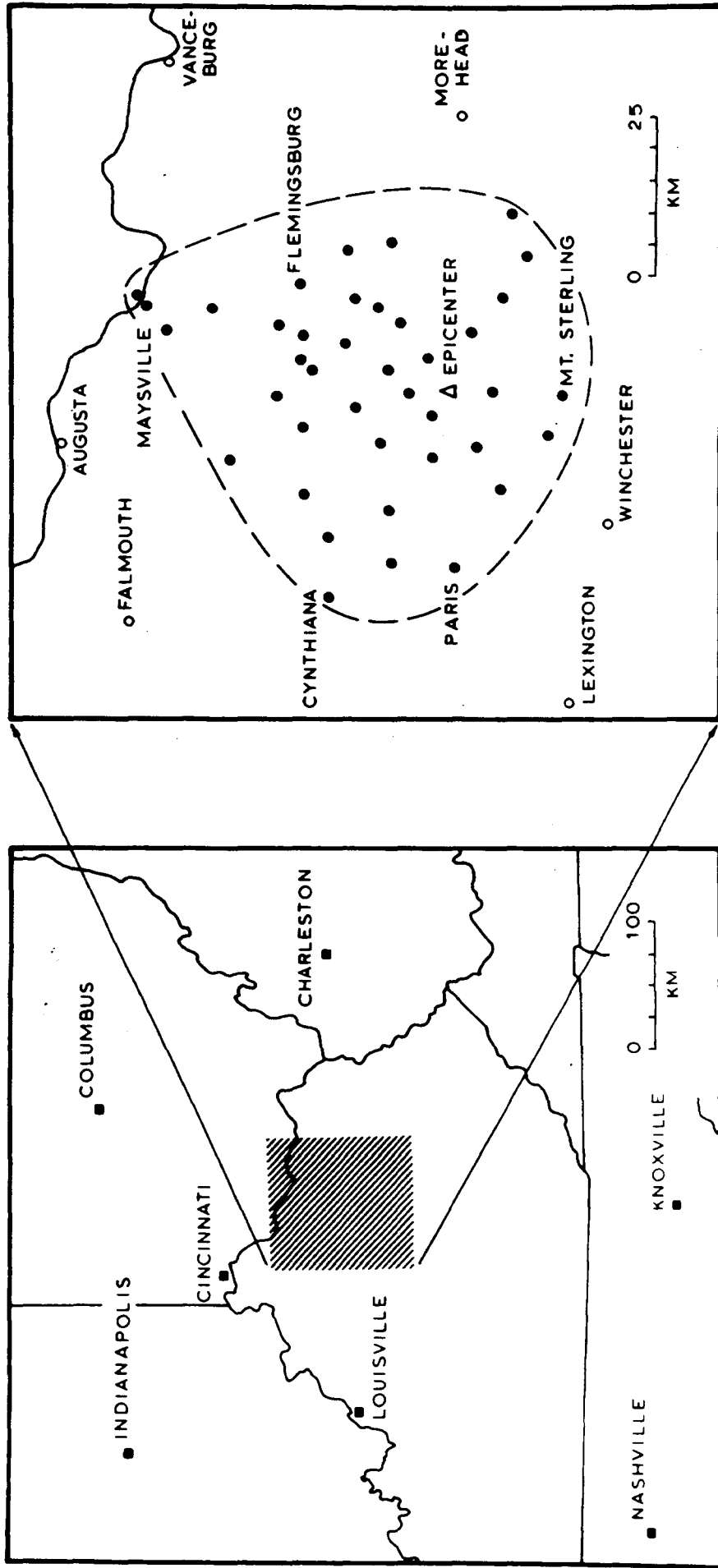


Figure 1. Meizoseismal area of the July 27, 1981 Sharpsburg, KY earthquake. Epicenter, at Sharpsburg, is represented by open triangle.

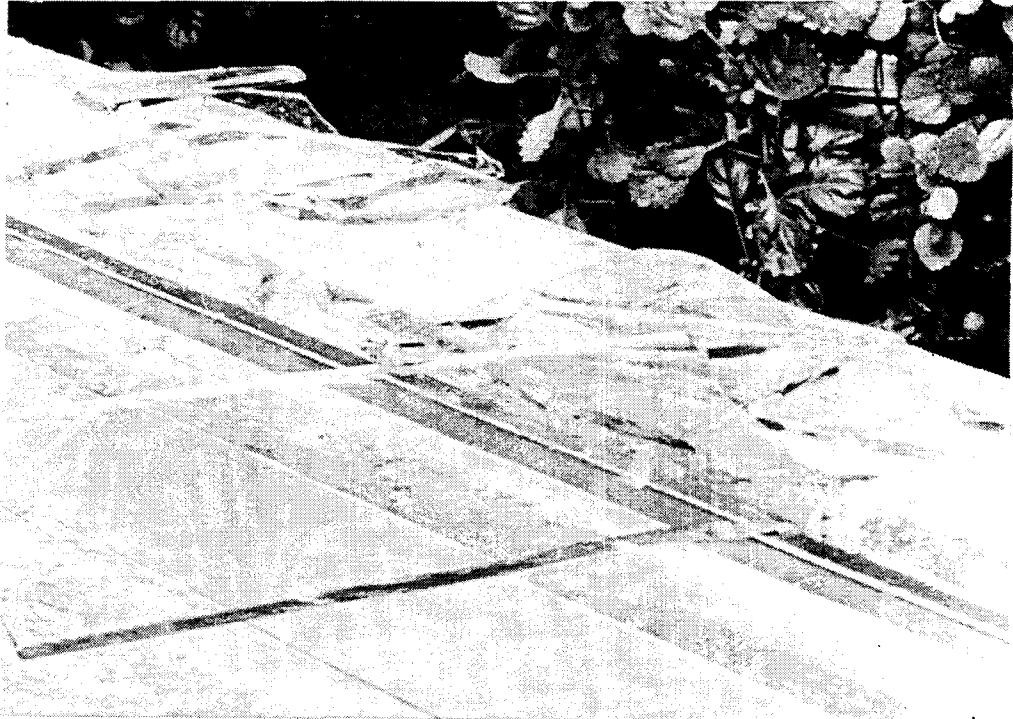


Figure 2. One-half inch broken plate glass bank window at street level in downtown Maysville. Photo by courtesy of J. Parker.



Figure 3. Brick fall from broken parapet in downtown Maysville, KY. Photo by courtesy of J. Parker.



Figure 4. Window cornice shaken loose from courthouse, in Flemingsburg, KY.

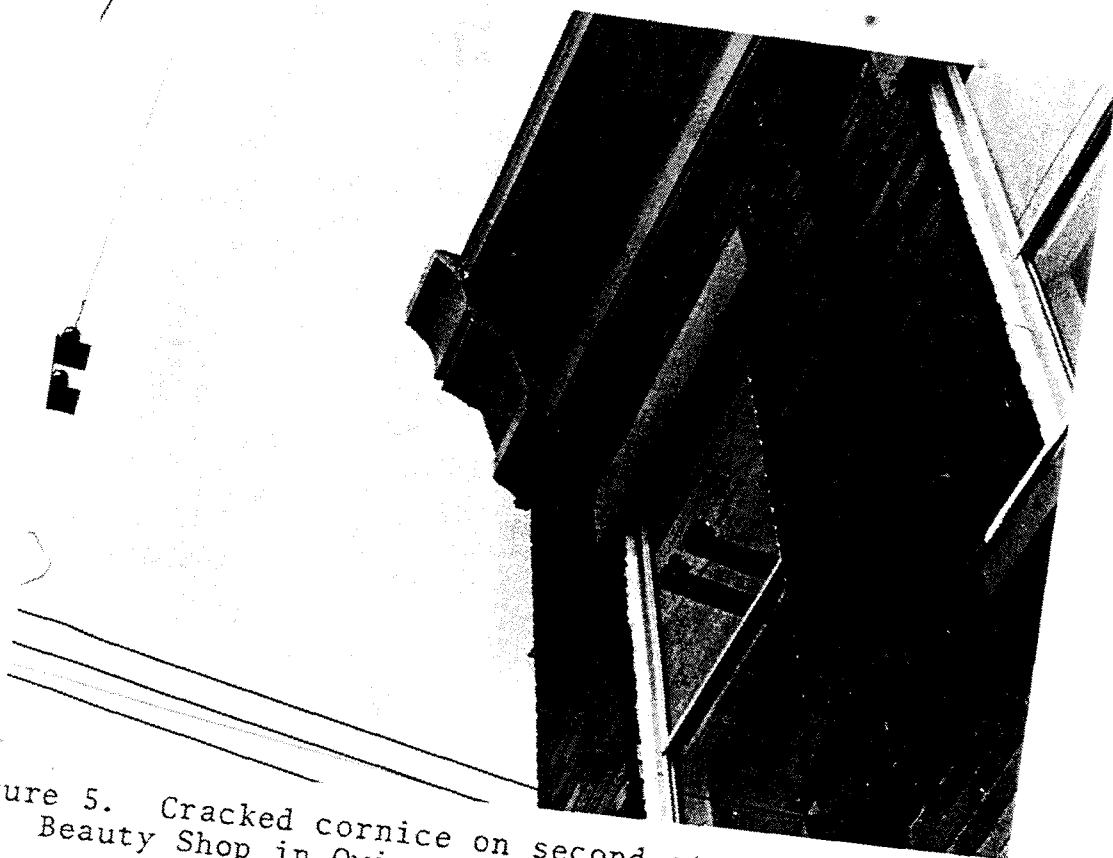


Figure 5. Cracked cornice on second story of Perfect Lady Beauty Shop in Owingsville, KY.



Figure 6. Chimney damage at Robert's residence in Sharpsburg, KY.



Figure 7. Broken chimney at the top of the west wall of the two story Toy residence near Sharpsburg, KY.



Figure 8. Typical chimney damage in downtown Maysville.
Photo by courtesy of J. Parker.



Figure 9. Chimney damage at abandoned residence on Route 11
south of Moorefield, KY.



Figure 10. Chimney damage at 152 Main Street, Owingsville, KY.



Figure 11. Chimney fall at one story frame structure at Sherburn, KY. Notice that the chimney has no flue for internal support, and that the mortar is in poor condition.



Figure 12. Chimney damage at Brewer residence on Route 11 north of Sharpsburg. Notice the condition of the mortar.



Figure 13. Chimney damage at two story frame Hall residence in Mt. Sterling. Notice poor condition of mortar.

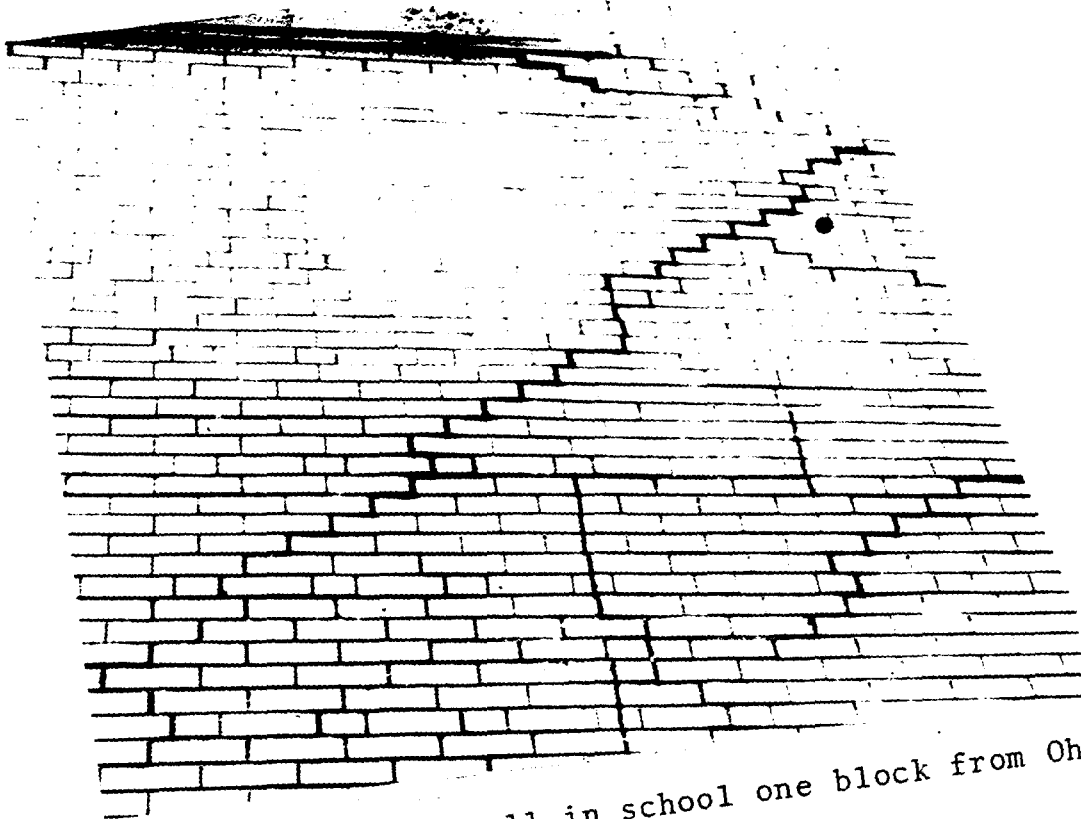


Figure 14. Cracked brick wall in school one block from Ohio River in Aberdeen, OH.

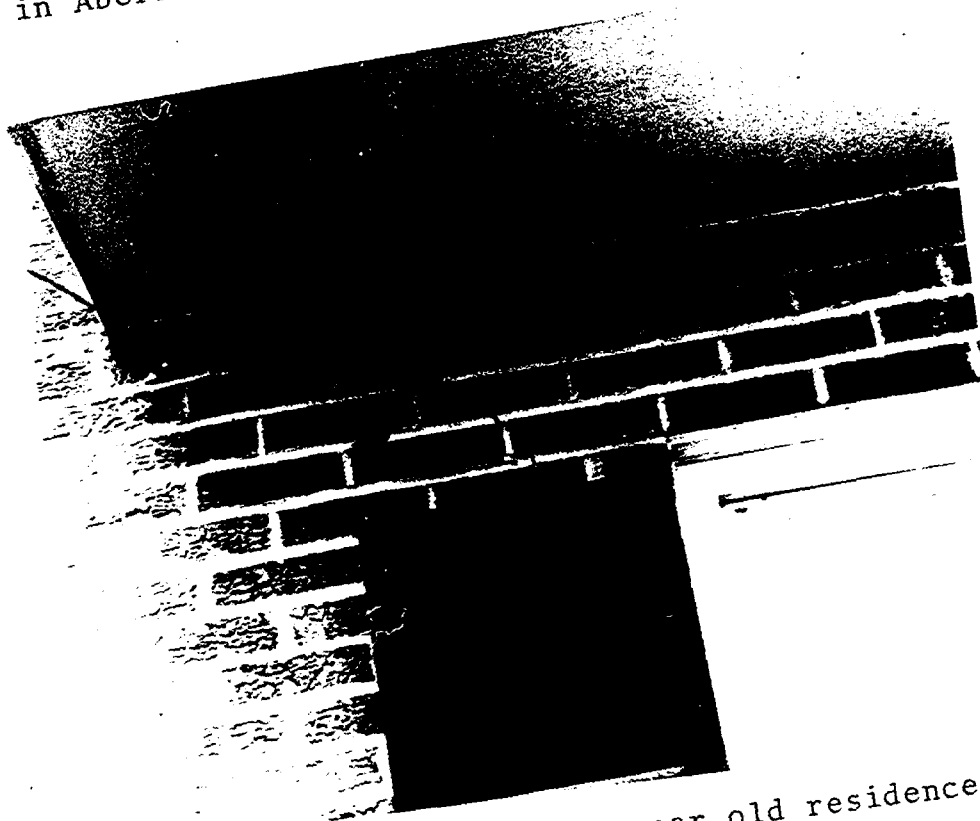


Figure 15. Cracked brick wall in six year old residence in Lewisburg, KY (see arrow).



Figure 16. Cracks in concrete block structure at golf course in Mt. Sterling, KY. Photo by courtesy of J. Zollweg.

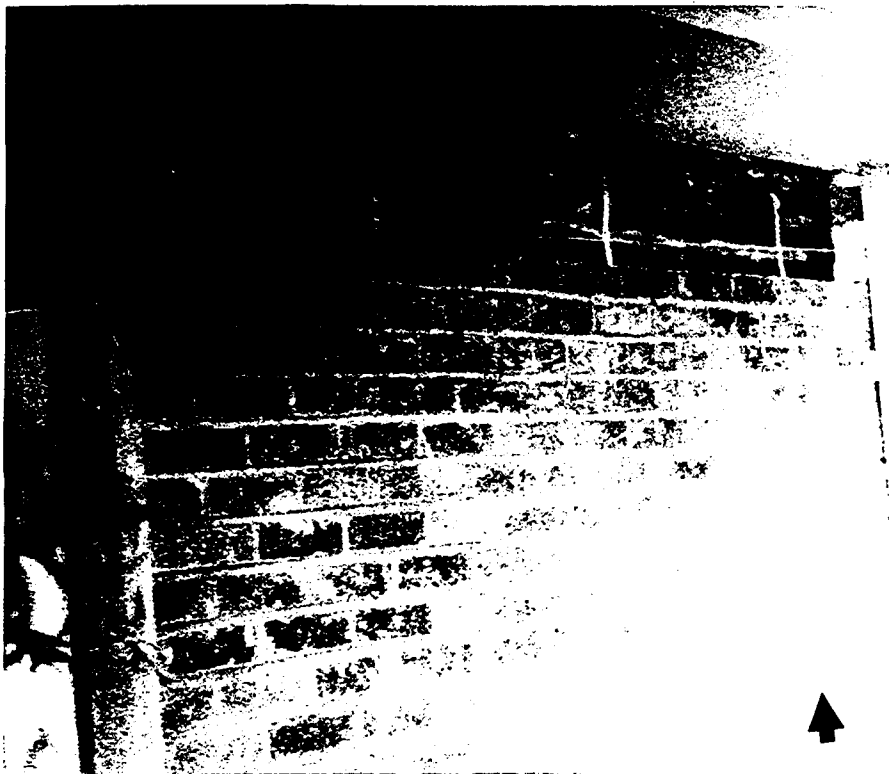


Figure 17. View of the rear of the Golden residence where brick veneer was shaken off down to the level indicated by the arrow. The structure is approximately 10 kilometers west of Sharnsburg, KY. and is two years old.



Figure 18. Same structure as shown in Figure 17, but view shows the front of the house where the brick veneer is pulled out from around the window frame (see arrow).



Figure 19. Cracked and bowed concrete block basement wall at Cooper residence in Flemingsburg, KY.



Figure 20. Cracked stairwell in the boiler room of the Fleming County Hospital in Flemingsburg, KY.

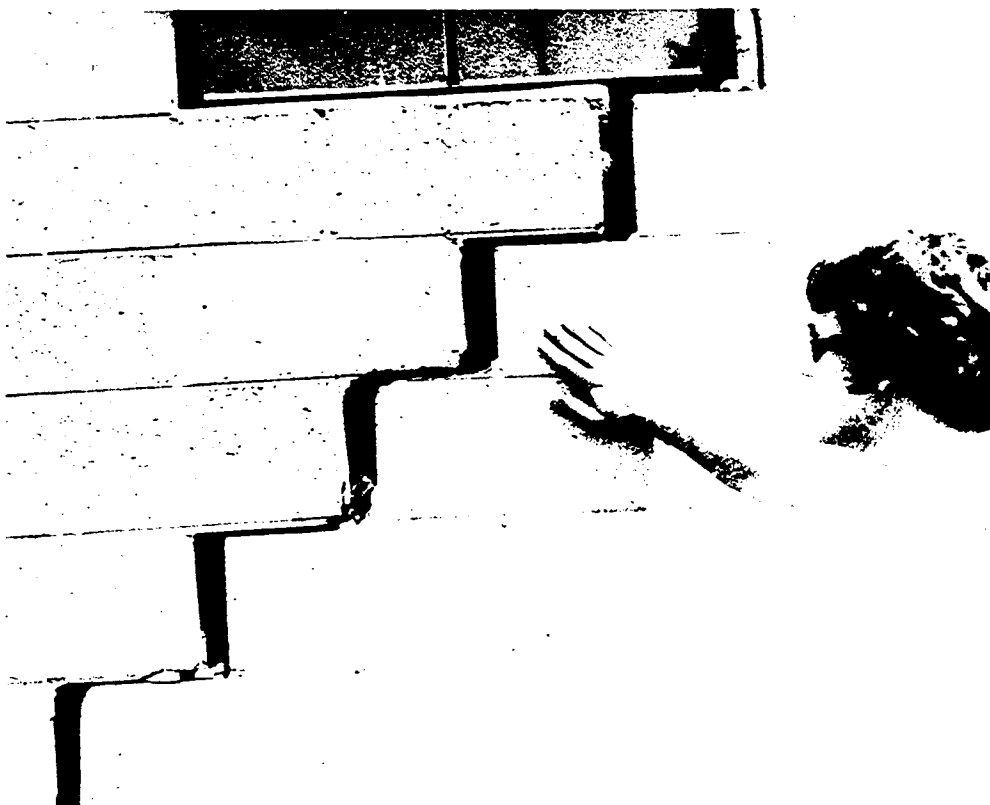


Figure 21. Cracked and separated exterior wall of the Morning Star Baptist Church in Owingsville, KY.



Figure 22. Displaced near pillar in the basement of the Morning Star Baptist Church in Owingsville, KY (see arrow).



Figure 23. Extensive cracking in the 150 year old brick Purvis home on the outskirts of Sharpsburg, KY.

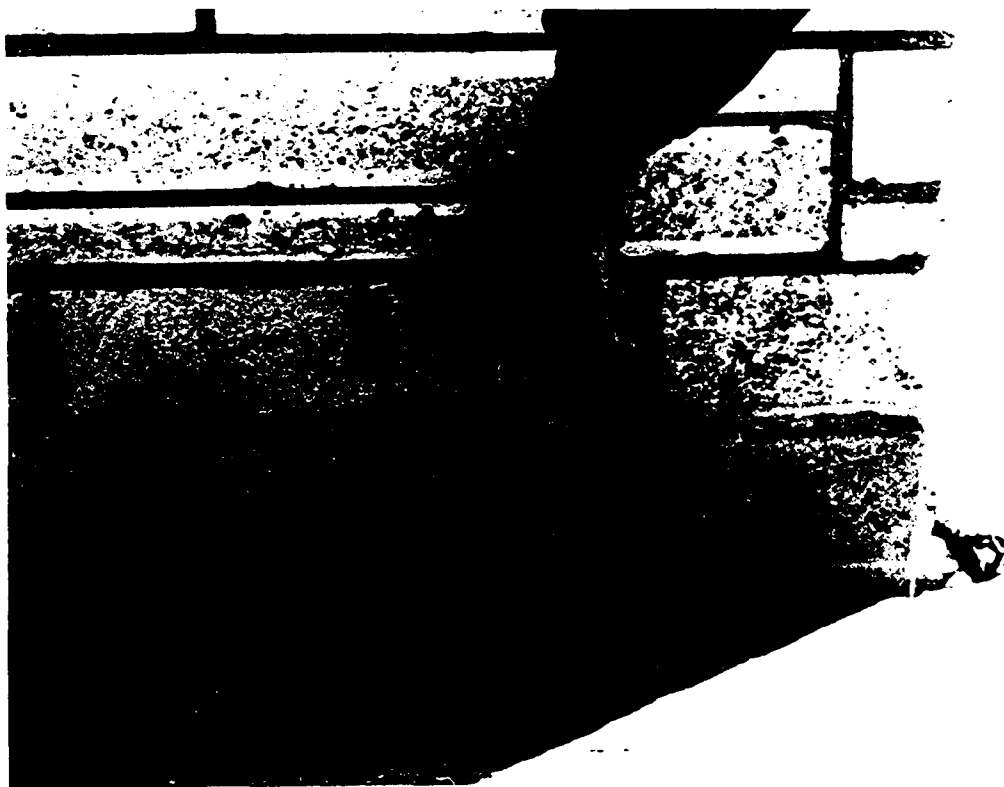


Figure 24. Cracked foundation in the poolhouse at Blue Lick State Park, KY.

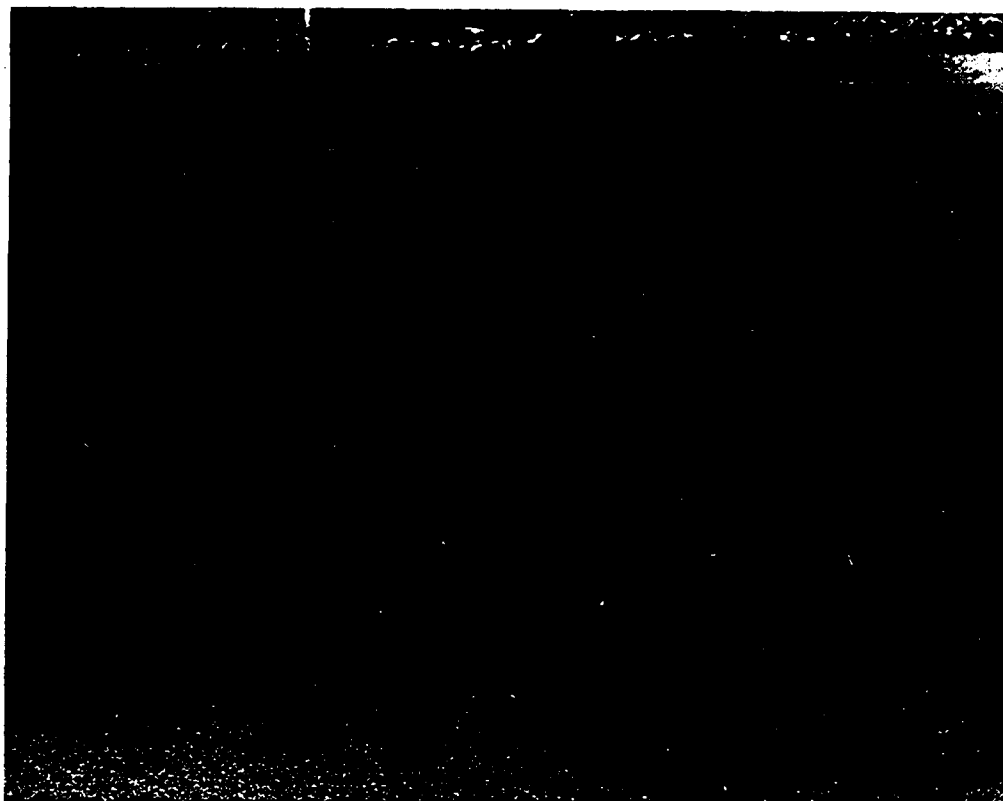


Figure 25. Cracked cement pool deck, believed to be caused by settling of manmade fill, at Blue Lick State Park, KY.

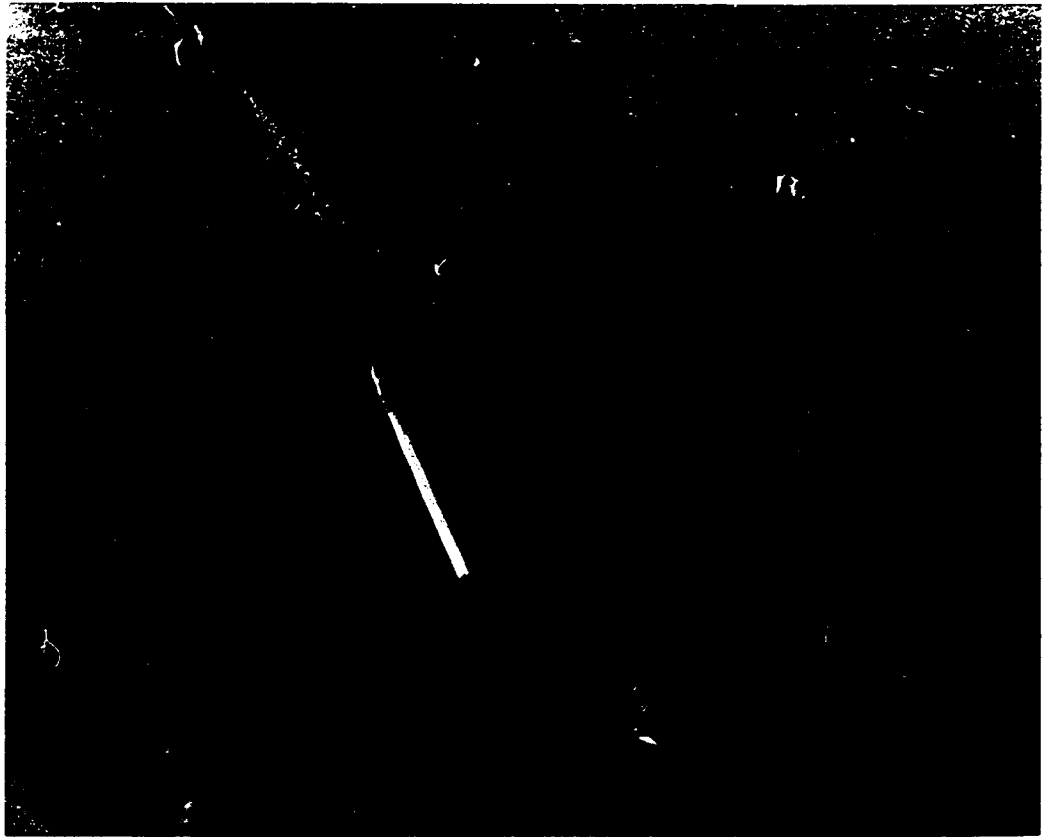


Figure 26. Cracked cement floor of a picnic shelter at Blue Lick State Park, KY.



Figure 27. Separation of fireplace mantle from wall at the Carpenter residence near Judy, KY. Photo by courtesy of TVA.

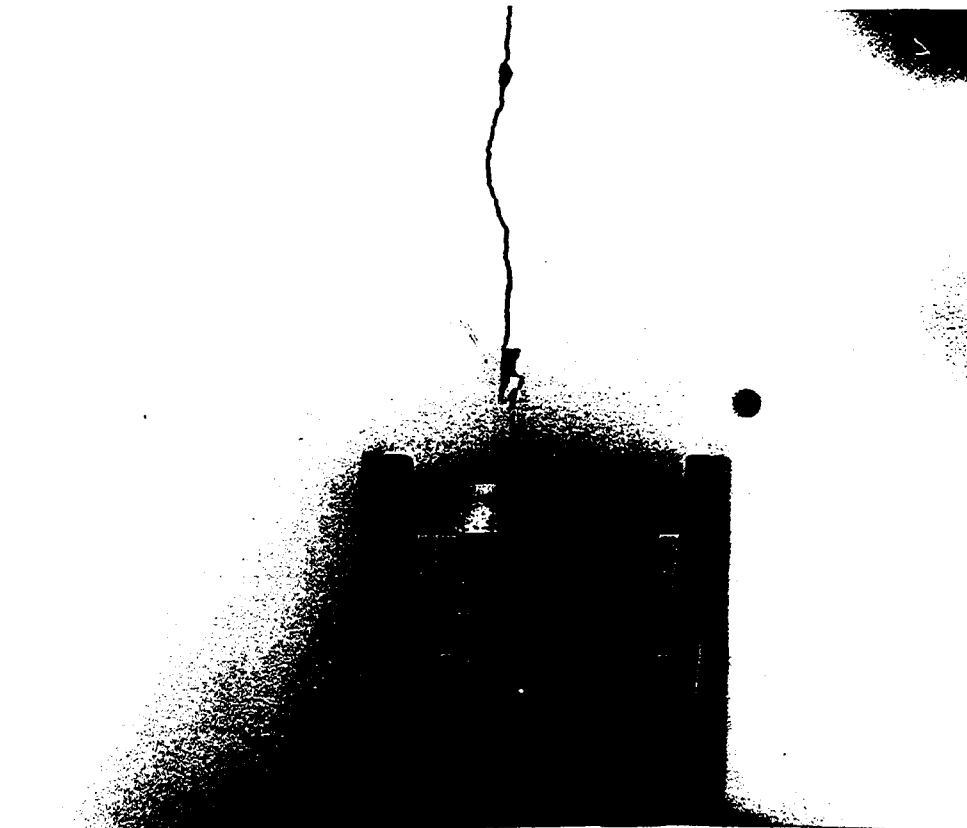


Figure 28. Plaster crack in second story bedroom of the Clay residence near Sharpsburg, KY.



Figure 29. View of the west wall of the Toy structure near Sharpsburg, KY. Notice how the wall is bowed inwards (see arrow); east wall of the structure was bowed outwards in a like manner.



Figure 30. Cracked cement block well house on the Toy farm near Sharpsburg, KY.



Figure 31. Broken 1 inch water pipe in cellar of well house on the Toy farm near Sharpsburg, KY. Broken water pipe was attached to a free standing four foot tall by two foot diameter water tank that was knocked over by the earthquake.

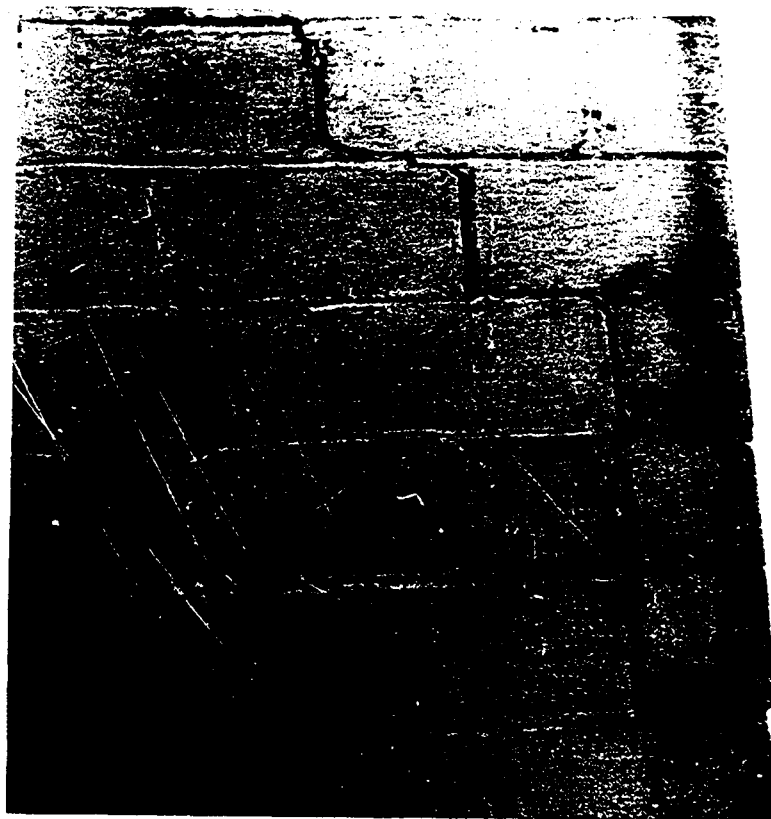


Figure 32. Crack in concrete block sidewall of the two story garage on the Toy farm near Sharpsburg, KY. The structure is built on the west slope of a hill, and the rear wall of the structure was shifted down slope.



Figure 33. Workman repairing the damaged limestone foundation of the Stull residence near Sharpsburg, KY. This section of the foundation was badly cracked, and displaced by as much as eight inches as result of the earthquake. Photo



Figure 34. View of the torn wallpaper along the corner of the first floor east end room of the Stull home near Sharpsburg, KY. Photo by courtesy of Mrs. R. Stull.



Figure 35. Damaged exterior south wall of the middle school in Mt. Sterling, KY. One window was removed and bricked in, as was the stone lintel over the window to the right (see arrows).



Figure 36. Damaged to one of several window pillars on the second floor of the middle school in Mt. Sterling, KY.

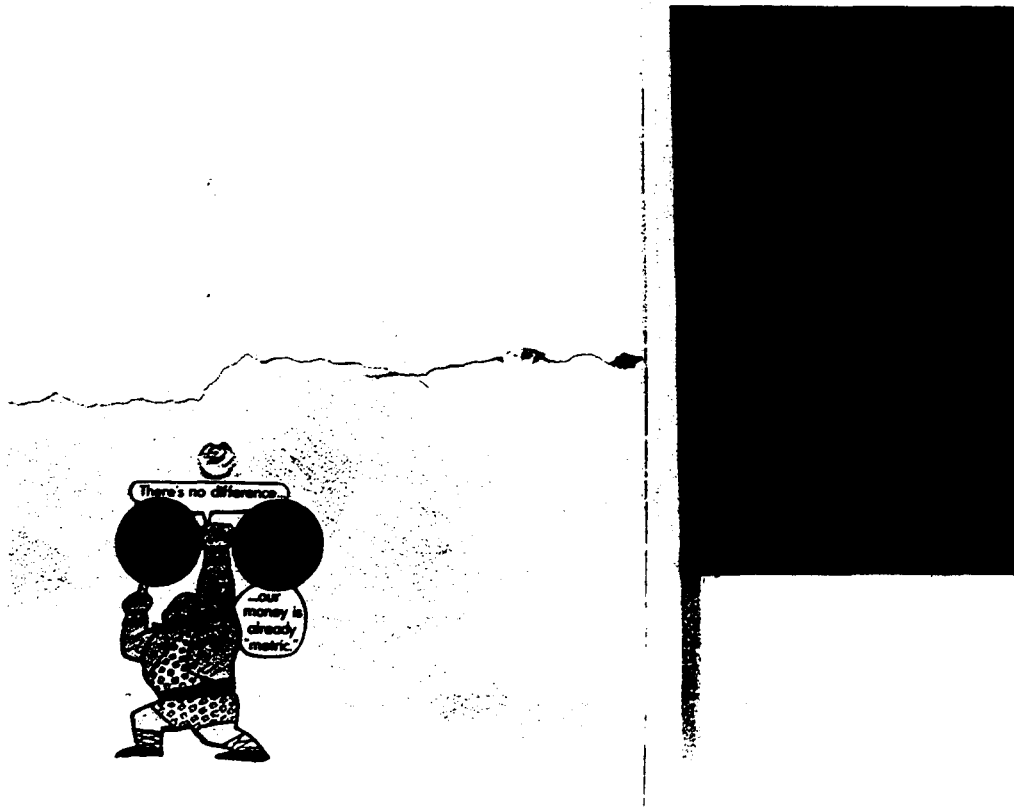


Figure 37. Typical damage to the interior of the north wall on the second floor of the middle school in Mt. Sterling, KY.

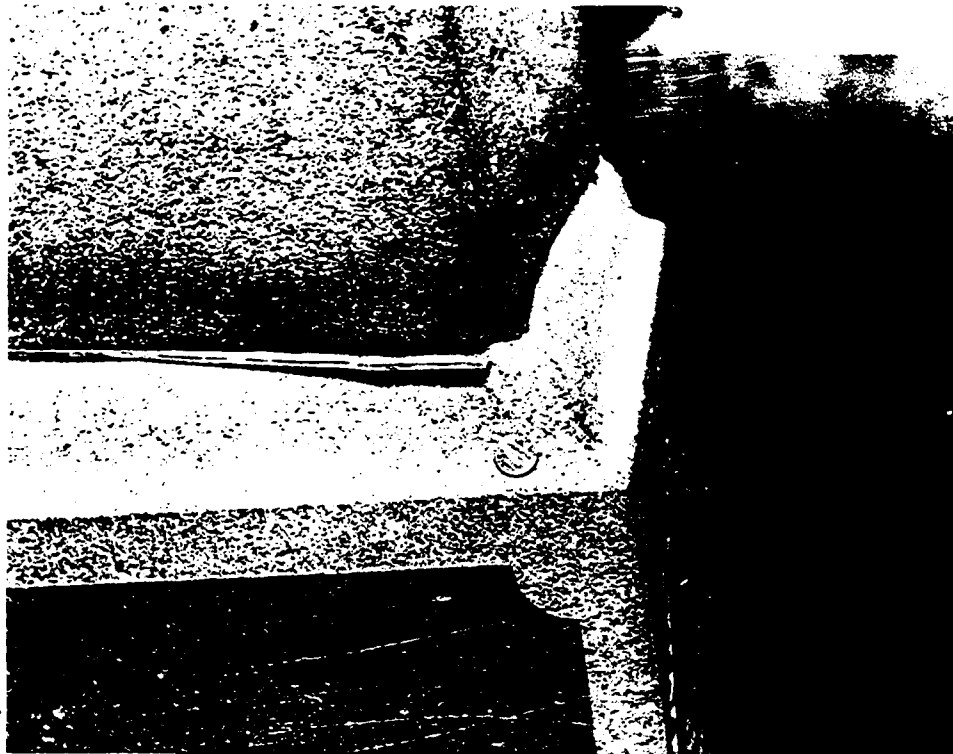


Figure 38. Clockwise rotation of stone monument in the Sharpsburg cemetery - penny for scale.

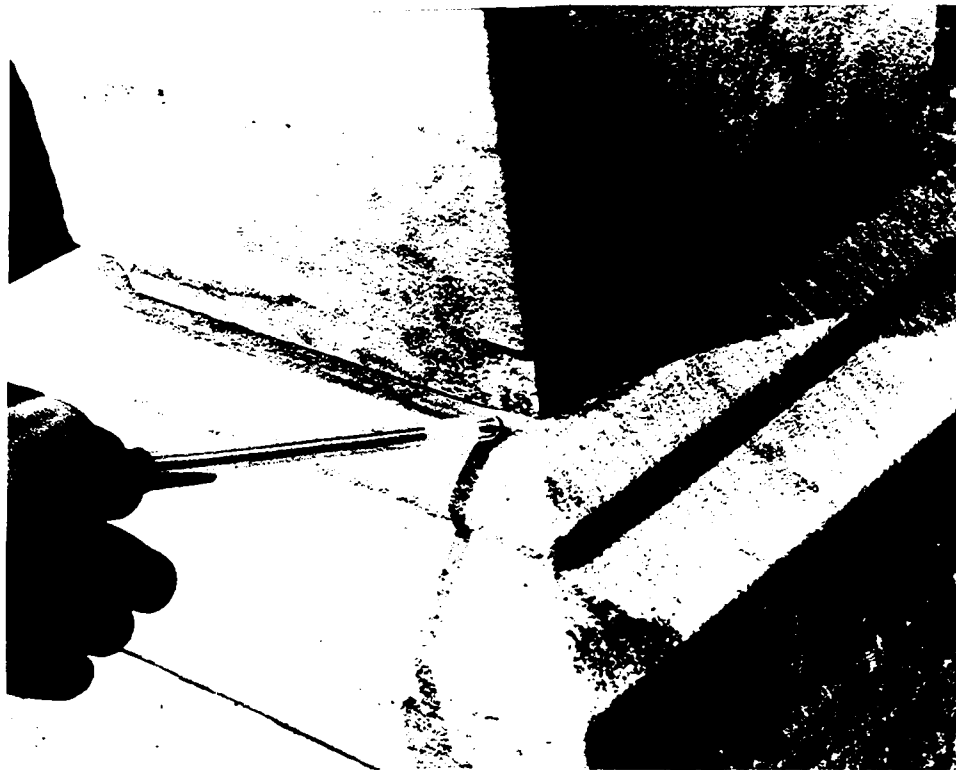


Figure 39. Example of stone monument in the Sharpsburg cemetery that was shifted approximately $3/4$ of an inch.



Figure 40. Example of a tombstone in the Sharpsburg cemetery that would have fallen if not for the metal rods connecting the top to the base.

Figure 44. Map illustrating the changes in well water levels (+ for increase flow; - for decrease flow), and muddied water (M) as a result of the earthquake.

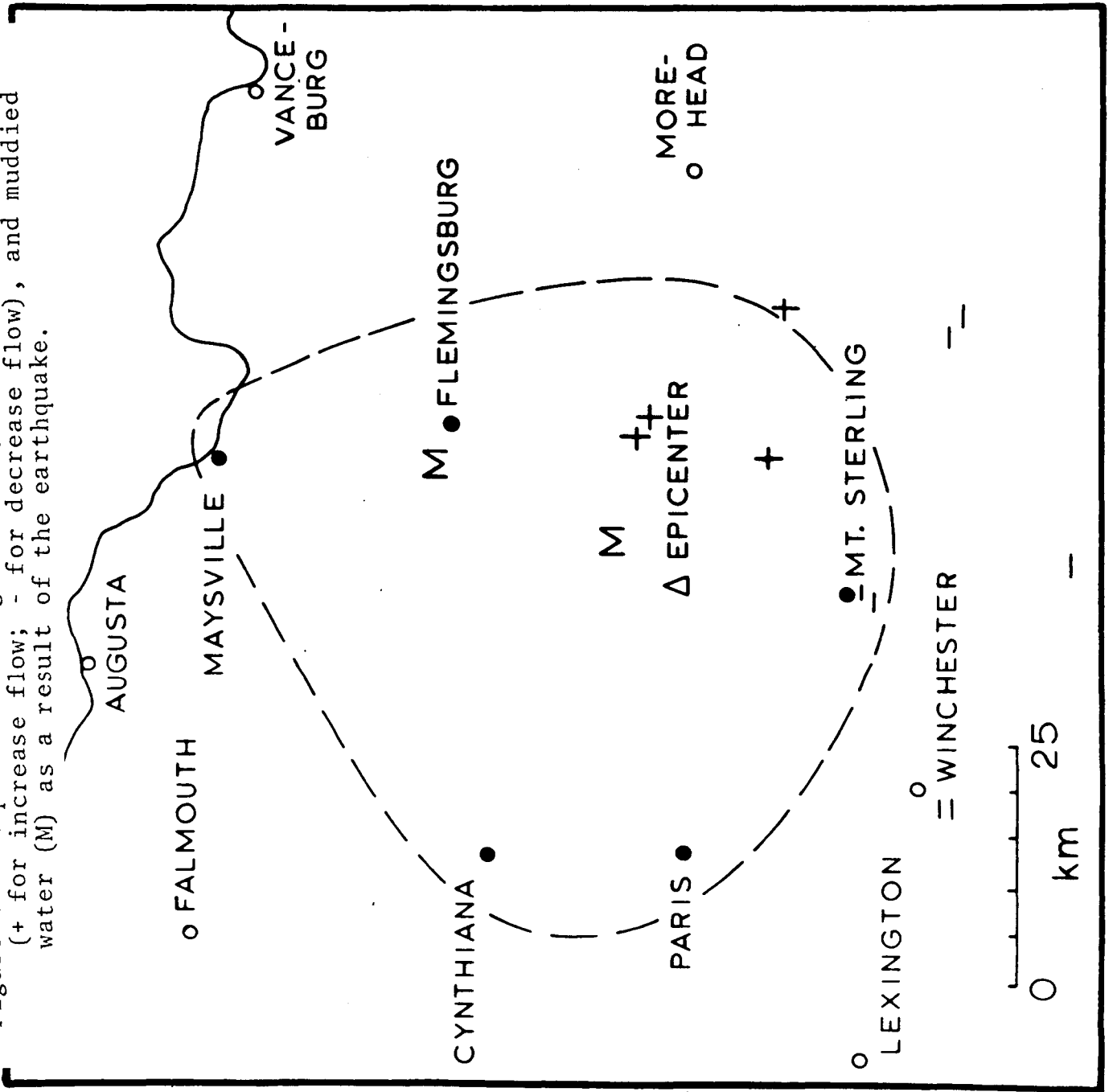


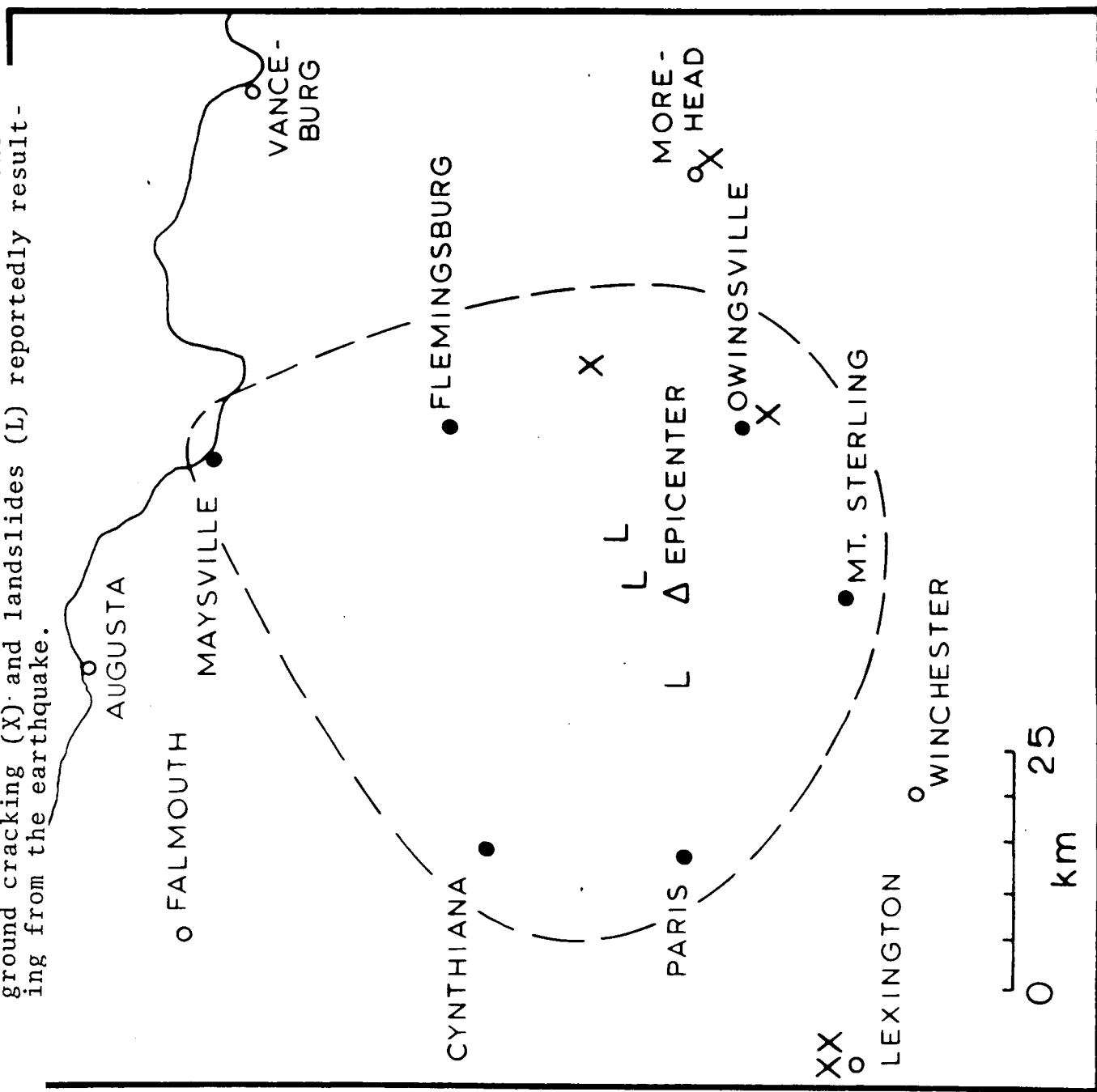


Figure 42. Ground cracking in Owingsville, KY that is believed to be desiccation cracks triggered by the earthquake. Pen for scale.



Figure 43. Small rockslide in roadcut near the Nicholas Co.-Bourbon Co. line that was triggered by the earthquake.

Figure 41. Map illustrating the distribution of some of the ground cracking (X) and landslides (L) reportedly resulting from the earthquake.



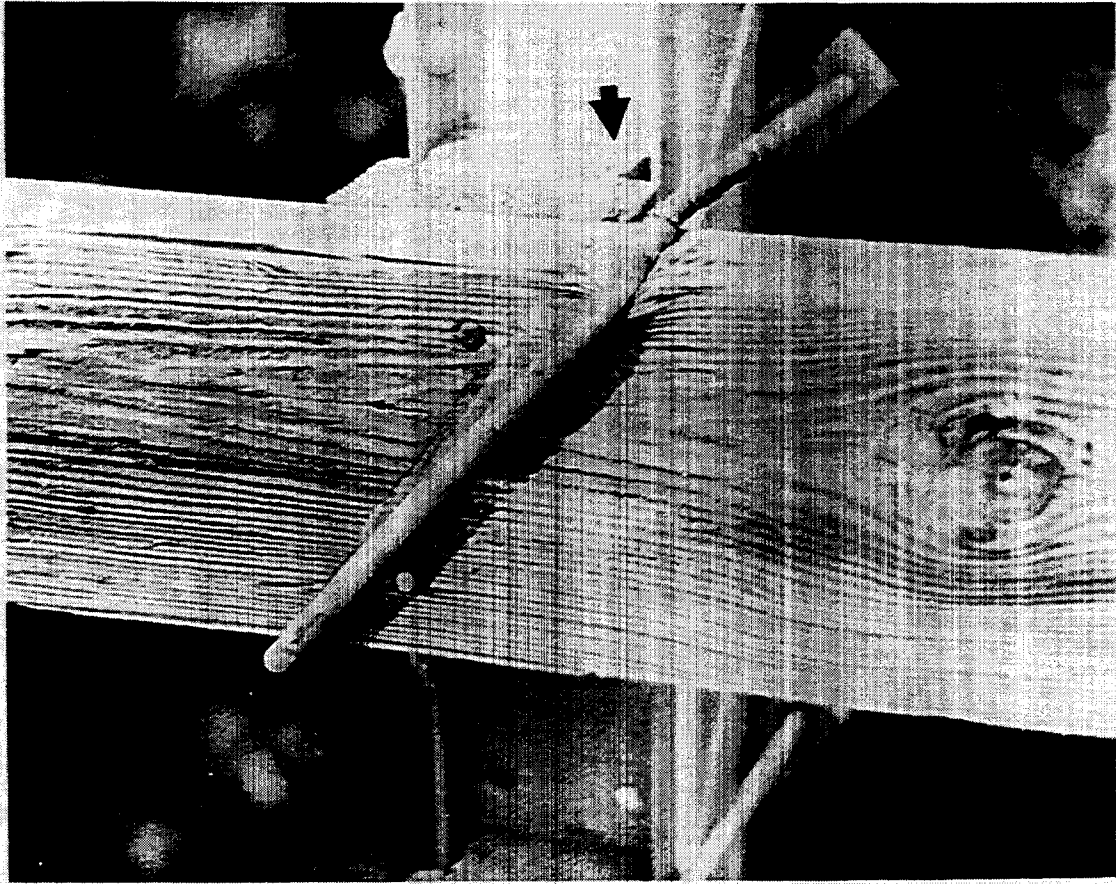


Figure 45. View of a broken and twisted tie-in rod observed on a small bridge on the Nicholas Co.-Bourbon Co. line (see arrow; half dollar is used for scale).

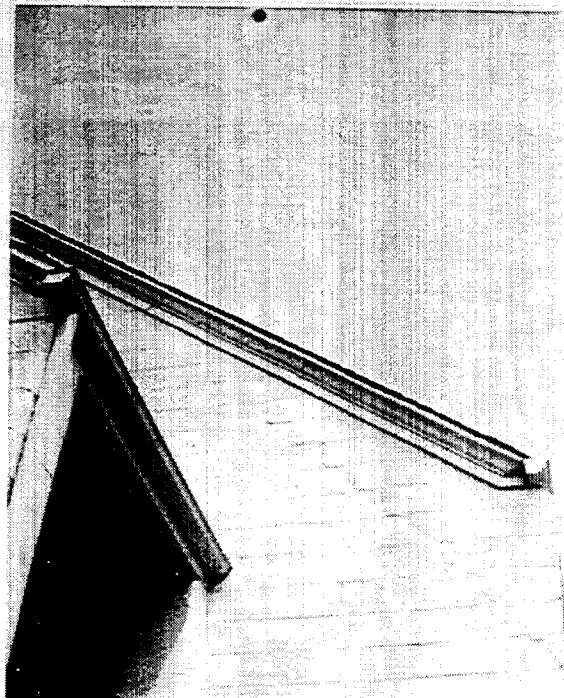


Figure 46. Previously cracked concrete block wall in the Calvary Baptist Church in Maysville, KY that was reopened by the earthquake. Photo by courtesy of TVA.

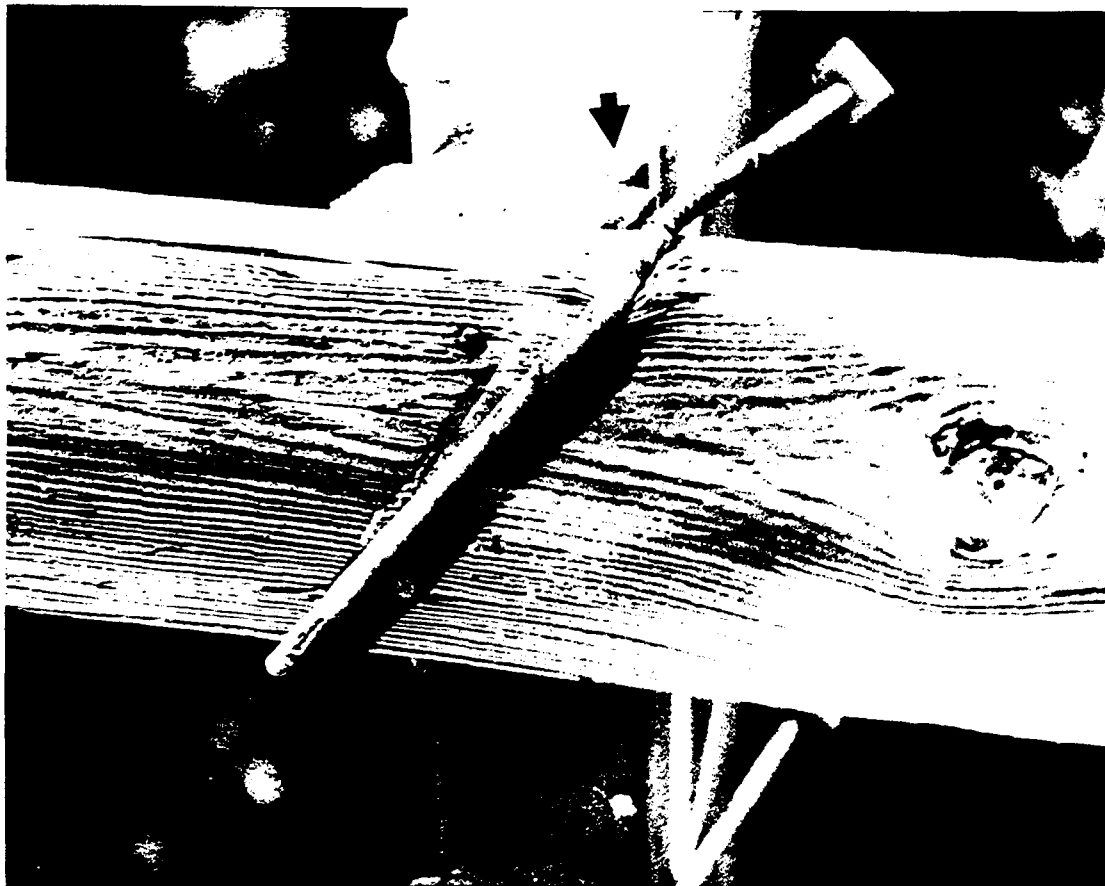


Figure 45. View of a broken and twisted tie-in rod observed on a small bridge on the Nicholas Co.-Bourbon Co. line (see arrow; half dollar is used for scale).

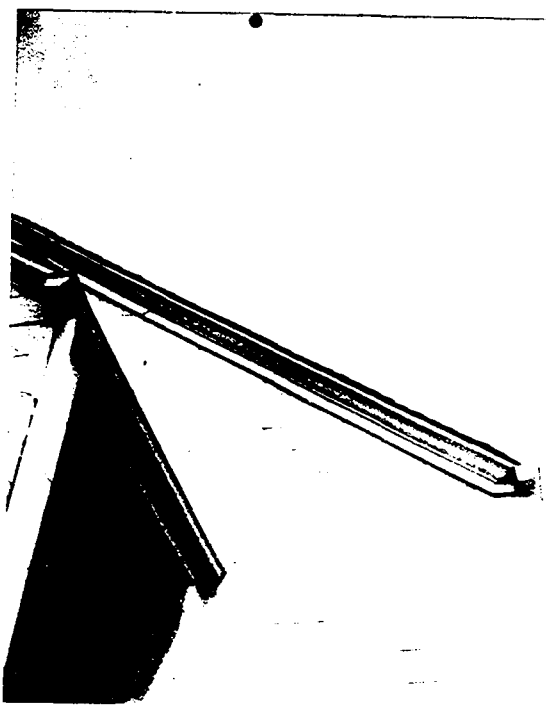


Figure 46. Previously cracked concrete block wall in the Calvary Baptist Church in Maysville, KY that was reopened by the earthquake. Photo by courtesy of TVA.

APPENDIX A: DAMAGE SUSTAINED IN MAYSVILLE, KY AS A RESULT OF THE JULY 27, 1980 EARTHQUAKE

Structures damaged in Maysville by the July 27, 1980 earthquake were primarily older buildings (pre-1930) multi-story structures, and concentrated in the three areas of town outlined by the dashed lines in Figure A1. Throughout the remainder of Maysville, as well as within the residential areas to the east and west of the town that are built along the same alluvial flood plain that underlies Maysville, were scattered instances of broken windows, minor chimney damage, and instances of cracking along the joints in brick walls.

The following summary is a list of the specific damage observed in the areas outlined by the dashed lines in Figure A1.

1. Structures within area A of Maysville sustained the greatest damage. St. Patrick's Church, located at the corner of East Third and Limestone Streets sustained extensive plaster cracks, toppled chimneys, and the cracked lintel shown in Figure A2; during the earthquake the church bells were heard ringing. The church was built in the late 1800's, remodeled ten years ago, and sits on level ground.

Adjacent to the church, the five year old gymnasium ceiling of St. Patrick's School separated from the wall and partially collapsed.

Along East and West Fourth Streets between Sutton and Limestone Streets, numerous instances of

plaster damage, broken and twisted chimneys, and cracked brick walls were observed. The front walls of one house, that was apparently in a poor state of repair prior to the earthquake, were bowed outwards and extensively cracked. In contrast, the wood frame houses along the southside of Fourth Street were, with exception to their chimneys, not noticeably damaged.

Hayswood Hospital, which is situated on the side of a steep hill on the southside of Fourth Street, consists of an older section in front built in 1911, and a newer addition in back that was built about ten years ago. Damage to the hospital consisted of interior plaster cracks in the front section as well as lateral displacements of up to 1 inch at the joints between the sections of the front columns shown in Figure A3. The newer back part of the hospital remained undamaged.

Across the street from the Mason County Court House located near the intersection of Catholic Alley and East Third Street, a section of an old stone fence moved downhill about five inches, while another section separated from an adjoining garden house. At the First Presbyterian Church, which is adjacent to the court house, one inch thick glass planes were cracked on the ground floor, and four large north-south orientated cracks were visible in the ceiling

plaster (new in April) on the upper floor.

The most severe damage in area A, and in fact in Maysville, was along Sutton Street. Brick walls in the older homes were extensively damaged, as were the majority of chimneys.

2. In the west end of Maysville within the area designated as B in Figure A1, numerous examples of chimney damage were observed, as well as one instance of a stone fence that had been shifted downhill about four inches. The houses in this section of Maysville are some of the oldest in town.
3. The third area in Maysville that sustained numerous instances of damage, is the area outlined in Figure A1 on the east end of town and designated by the letter C. The homes in this section are generally newer than those in areas A and B, and instance of damage were fewer and less severe. Nevertheless, this area sustained widespread minor chimney damage, and numerous instances of broken glass.

FIGURE CAPTIONS FOR APPENDIX

Figure A1. City map of Maysville, KY. The shaded sections identified by the capital letters are referred to in the text of the Appendix.

Figure A2. Cracked door lintel in St. Patrick's Church on W. 3rd Street in Maysville, KY. Photo by the Courtesy of TVA.

Figure A3. Columns at the front of the Hayswood Hospital in Maysville, KY that were displaced by as much as one inch at the joints.

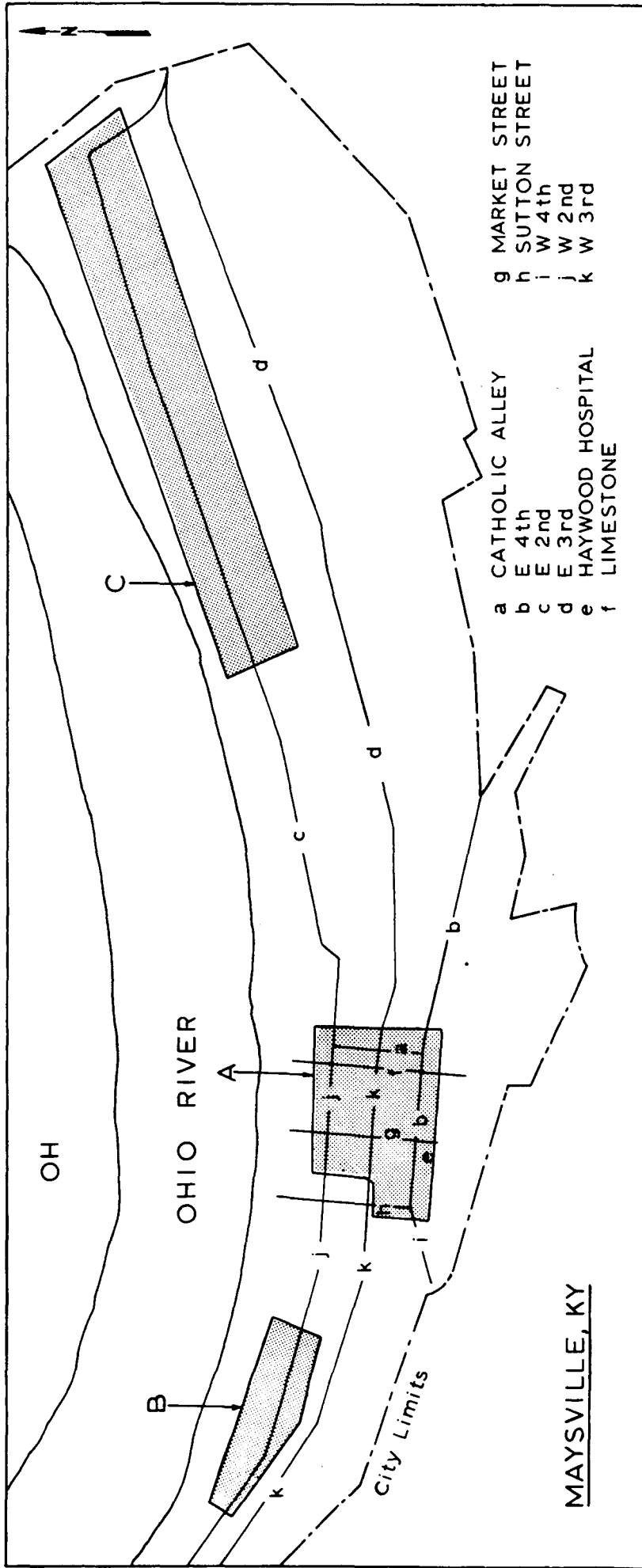


Figure A1. City map of Maysville, KY. The shaded sections identified by the capital letters are referred to in the text of the Appendix.



Figure A2. Cracked door lintel in St. Patrick's Church on W. 3rd Street in Maysville, KY. Photo by the Courtesy of TVA.



Figure A3. Columns at the front of the Hayswood Hospital in Maysville, KY that were displaced by as much as one inch at the joints.

The Sharpsburg, Kentucky Earthquake of July 27, 1980

Robert B. Herrmann, Charles A. Langston

and James E. Zollweg*

ABSTRACT

The Sharpsburg, Kentucky earthquake was the second largest earthquake to have occurred in the U.S., east of the Continental Divide, in the past twenty years, having a seismic moment of 4.1×10^{23} dyne-cm. A surface-wave focal mechanism study defines a nodal plane striking N30°E, dipping 50°SE and a nearly vertical nodal plane striking N60°W. P-wave first motion data indicate right-lateral motion on the nodal plane striking N30°E, with the pressure axes oriented east-west. These angles can be varied by $\pm 10^\circ$ without affecting the fit to the surface wave data. The surface-wave solution is reinforced by a modeling of long-period seismograms at regional distances.

The P, pP and sP polarities and amplitudes from the short period vertical component array stack at NORSAR are used together with six unambiguous short period P wave first motions recorded in North America to test whether it is possible to constrain focal mechanism solutions with such data. These solutions are compatible with the surface wave solution. Waveform modeling of the NORSAR data suggests a source pulse duration of 1.0 seconds and constrains the depth to 12.0 km. To match m_b estimates from

*Present address: Geophysics Program AK-50, University of Washington, Seattle, WA 98195.

NORSAR and Canadian stations, t^* , for teleseismic P, must be 0.7 and 0.5, respectively, when the synthetics are scaled using the surface wave seismic moment.

In spite of extensive coverage of the epicentral zone, fewer than 70 aftershocks were recorded. The largest aftershock had an $m_{blg} = 2.2$. Aftershock locations suggest that the nodal plane striking N30°E is the fault plane. An aftershock area of 30-50 km² implies a stress drop of 2.8-6 bars and a dislocation of 2.0-3.4 cm.

Because of the variety of studies performed, this earthquake is presently the best studied eastern North American seismic event with well constrained estimates of focal depth, focal mechanism and seismic moment and indications of the duration of the source time function and upper mantle P-wave t^* .

INTRODUCTION

The Sharpsburg, Kentucky earthquake occurred at 18:52:21.8 UT on July 27, 1980 and was located at 38.17°N, 83.91°W with a focal depth of 8 km (NEIS). NEIS gave magnitude estimates of $m_b = 5.2$ and $M_S = 4.7$. Using regional phases, Mauk *et al* (1982) gave the coordinates 38.18°N and 83.94°W and a focal depth of 15 km for the earthquake. In reviewing the earthquake history of the region, Reagor *et al.* (1981) noted that the earthquake occurred in an area of low seismic activity, with no equivalent sized earthquake having occurred within 200 km. Because of its size, its unexpected location, and because it was well-recorded, a number of different types of analysis of the main shock and aftershocks were performed in order to estimate the focal depth, focal mechanism, seismic moment and spatial distribution of aftershocks.

MAIN SHOCK SOURCE STUDIES

Several focal mechanism studies were performed on the main shock. Mauk *et al* (1980) used regional and teleseismic P-wave observations to obtain a focal mechanism consisting of a nodal plane striking N 16° E, dipping 56° E with a slip angle of 232°. Because this focal mechanism differed substantially from the ones obtained from regional surface wave and teleseismic body waveform studies discussed in the present paper, Mauk *et al* (1982) reexamined their data, finding errors in some of the seismograph station polarities. Using the corrected data set, they obtained a focal mechanism consisting of a nodal plane striking N 42° E, dipping 50° E with a slip angle of 184°. This section discusses the surface wave and body waveform analysis of this earthquake.

Surface Wave Studies.

The focal mechanism, focal depth and seismic moment were estimated using the techniques described by Herrmann (1979). The Central United States earth model of Table 1 and the surface-wave anelastic attenuation coefficients of

Herrmann and Mitchell (1975) were used for the inversion of the surface-wave data. Rayleigh wave spectral amplitude data in the period range of 6 to 45 seconds were obtained from the eighteen seismograph stations SCH, OTT, MNT, STJ, WES, BLA, SHA, EPT, LUB, ALQ, FVM, SLM, DUG, COR, PNT, FFC, YKC and FCC to yield a total of 237 spectral amplitude-period pairs for analysis. Love-wave data in the period range 6 to 50 seconds yielded 223 spectral amplitude-period pairs from the seventeen seismograph stations SCH, OTT, MNT, STJ, WES, BLA, SHA, EPT, LUB, ALQ, DUG, COR, PNT, SES, FFC, YKC and FCC.

After systematically searching through all possible focal mechanisms, the surface-wave amplitude spectra and P-wave first motion data were best fit by the focal mechanism given in Figure 1. The pressure axis trends at 251° and plunges at 21° while the tension axis trends at 349° and plunges at 21° . For these parameters one nodal plane strikes $N30^\circ E$ and dips 60° , while the other is vertical and strikes $N60^\circ W$. This focal mechanism is also parameterized by a strike, s , of 30° , a dip, δ , of 60° and a slip, λ , of 180° . Proceeding clockwise from north, the seismograph stations and their P-wave polarities are AAM(+), AN3(+), ALE(+), BV1(-), HWV(-), BLA(-), NAV(-), TKL(+), PWLA(-), WCK(-), DWM(-), RMB(-), ELC(-), DON(-), FVM(-), TYS(-), SLM(-), BLO(-), CHI(+), LHC(+), FCC(+), AN11(+), AN10(+), AN8(+) and AN1(+). For regional P-phases, the P-wave take-off angles of 47° and 49° were used for stations at distances greater than and less than 400 km, respectively. The surface-wave data were quite sensitive to the dip and strike of the nodal planes, so that these parameters are known to within $\pm 10^\circ$. Perhaps due to the nature of the focal mechanism, as well as the small number of spectral-amplitude pairs, the surface-wave data were not very sensitive to focal depth such that any focal depth between 14 and 22 km would fit the spectral amplitude data equally well. An acceptable value would be a focal depth of 18 km, for which the seismic moment is estimated to be 4.1×10^{23} dyne-cm. Fol-

lowing Herrmann (1979), the correlation coefficient between the observed and predicted Rayleigh-wave vertical component spectral amplitudes is $r_R = 0.734$, while for the Love-wave data it is $r_L = 0.666$. The focal depth of 18 km is indicated because r_R peaks at this depth. The seismic moment estimate increases with focal depth from 3.7×10^{23} dyne-cm at 14 km depth to 4.7×10^{23} dyne-cm at 22 km depth. The anelastic-attenuation-corrected, observed Rayleigh and Love wave data are compared to theoretical radiation patterns in Figure 2. The fits are excellent, as indicated by the large values of the correlation coefficients.

Regional Waveform Studies.

Because of the distribution of excellent first motion data, there is no problem in defining the compressional and dilatational quadrants of the focal mechanism. An independent test of the correctness of the solution could be obtained by computing observed and predicted surface-wave phases at selected stations for a range of periods. In order to do this, the seismograph stations must be at relatively short epicentral distances so that imperfect knowledge in phase velocity do not affect the comparison of phases. Another way to perform this test is to compare actual and predicted waveforms rather than spectral phases.

Using the approach used by Herrmann *et al.* (1980), a point source dislocation source with focal mechanism given by Figure 1 and a seismic moment of $4.1E + 23$ dyne-cm was placed at depths of 11, 15 and 20 km in the Central U.S. earth model of Table 1. A parabolic source time function with duration of 1.0 second was used for the synthesis. The numerical seismograms were obtained by performing a double Fourier, Fourier-Bessel transform over the frequency range 0-2 Hz and over the phase slowness range 0-2.0 sec/km. The resultant time histories were passed through a numerical realization of a 15-100 WWSSN long period seismograph with a peak magnification of 3000.

Figure 3 shows the observed and predicted vertical component seismograms at Saint Louis, Missouri, SLM, a distance of 555 km from the earthquake along an azimuth of 277° . Except for the rippling motion after the first part of the surface wave, the waveforms and amplitudes agree well, especially the first ten seconds of the surface wave arrival. The lack of depth resolution is similar to that inferred from the spectral amplitude study. Figure 4 presents the observed and predicted three component seismograms for three depths at Blacksburg, Virginia, BLA, a distance of 325.9 km along an azimuth of 109° from the earthquake. A non-linear spring resonance effect is seen in the vertical component record. The sense of motion and amplitudes of the observed and predicted traces are in good agreement. The SH motion on the horizontal components matches the observed traces well if the predicted trace is shifted two seconds later. However, this time shift will not yield a good match of the Rayleigh wave motion on the vertical and east-west traces. The relative amplitudes of the three components can be adjusted by slightly modifying the focal mechanism since BLA lies near both Rayleigh and Love wave nodal planes (Fig. 2).

In comparing the synthetic time histories generated for the same source but at depths of 11 and 20 km, the fine character of the SH arrivals changes, but the time separation between the SH and Rayleigh wave arrivals did not change. The propagation path between the epicenter and Blacksburg, VA is perpendicular to the Appalachian Mountain front, with the depth to the Precambrian changing from about 1 km at Sharpsburg to 5+ km in eastern Kentucky. This indicated that the Central U.S. earth model is certainly not applicable for that path.

Multiple-filter analysis (Dziewonski *et al.*, 1969) was used to study the Rayleigh and Love wave dispersion to BLA. In an attempt to match the group velocity, the upper layer of the Central U.S. earth model was increased in thickness.

The resulting Appalachian Basin model is given in Table 1. A suite of seismograms was generated for a depth of 14 km in that model. This depth was chosen to be closer to the estimates from teleseismic body waveforms. The discrepancy between the observed and predicted Rayleigh and SH phases was not completely resolved.

The use of synthetic seismograms reinforced the surface wave P-wave first motion conclusions concerning the focal parameters. The observed seismograms were fit in their major characteristics, but as seen from the discussion of the BLA records, the problem of crustal structure is important. The quality of data was not sufficient to start a study of crustal structure.

Body Waveform Studies.

P waves from the Sharpsburg earthquake were large enough to be recorded at the NORSAR seismic array offering an unprecedented opportunity to accurately determine source depth for an Eastern U.S. earthquake by using teleseismic depth phases. Figure 5 displays 25 seconds of the short period waveform at NORSAR derived by summing the responses of each center element from each subarray. The surface reflections pP and sP are plainly visible as the prominent arrivals about 4.2 and 5.7 seconds after direct P, respectively. A depth of 12 km is obtained for the event using this timing information using standard travel time tables.

In addition to depth information obtained by the pP and sP observations, the amplitudes and polarities of pP and sP relative to direct P also offer independent constraints on the source mechanism. Unambiguous P-wave first motions allow considerable variation in the placement of the P nodal planes (Figure 6). To improve the body wave fault plane solution the polarities and amplitude of sP and pP relative to P at NORSAR were used in conjunction with unambiguous P first motions read from ALE(+), EDM(+), FCC(+), LUB(-), SCP(-), and

BLA(-), NORSAR(+).

A systematic testing algorithm was used to check the polarities of all phases and NORSAR sP/P and pP/P amplitude ratios against the orientation parameters strike, dip, and slip (Pearce, 1977; Langston, 1981). A successful mechanism was one which satisfied all polarities and which the amplitude ratios satisfied

$$\left| \frac{O_1 - C_1}{O_1} \right| \leq \sigma$$

where O_1 was an observed amplitude ratio, C_1 was a calculated ratio, and σ was set to 0.5. The response for sP and pP was calculated using ray methods outlined in Langston and Helmberger (1975) for crustal models in Table 2. Model A is a simple eastern U. S. model, Model B is a simple halfspace model, and Model C is a variation of Model A to take into account the effect of the sedimentary rock cover in the region of the epicenter.

Figure 6 shows the result of the testing procedure for several assumptions of input data and crustal models. Considerable variation in the mechanism is evident when only polarities (including pP and sP) are used. Inclusion of the NORSAR relative amplitudes serves to place important constraints on the mechanism. Where the polarities could allow oblique thrusting as a possible mechanism, the relative amplitude measurements exclude this possibility and suggest right-lateral strike-slip faulting on a NE striking plane dipping to the SE or left-lateral motion on a vertical plane striking to the SE. Changing the crustal model from model A to B only serves to increase the mechanism variability a small amount. Note the good agreement between this body wave mechanism and the mechanism obtained through the surface wave analysis.

Synthetic seismograms for the NORSAR sum were calculated for selected acceptable orientations and are shown in Figure 5. The NORSAR short-period

instrument response and a Futterman (1962) attenuation operator ($t^* = 1.0$) were included. Adding a lower velocity layer at the surface of crust A to produce crust C served to reduce the sP conversion somewhat, improving the relative amplitude behavior of this phase. Note the good agreement in phase timing and waveshape between observed and synthetic. This is all the more remarkable considering that the data are short-period. It was found that a triangular far-field time function with a rise time of 0.8 sec and a fall-off time of 0.2 sec fit the direct P waveform with respect to the small initial compression compared to the large dilatational backswing immediately after. Minimum phase or symmetric far-field time functions did not produce the large positive third swing seen in the data. A change of one km in depth is discernible as a time shift between the surface reflections and direct P in the synthetic waveforms. This can be taken as the uncertainty in the depth estimate. This independent determination of the source depth agrees with the lower range of the 14 to 22 km depths permitted by the surface wave modeling.

No particular significance should be attached to the exact shape of the time function or choice of the attenuation operator. These parameters serve only as a vehicle to provide a P pulse shape for use in testing the relative amplitudes of pP and sP to P in Figure 5. Numerical experiments with NORSAR and WWSSN short-period instrument responses do show, however, that pulse duration is related mainly to the duration of the time function with the amplitudes being a sensitive function of the attenuation. Using the seismic moment of 4×10^{23} dyne-cm determined from the surface waves and the time function determined from the NORSAR P wave, an estimate of average t^* may be made by comparing synthetic and observed m_b values. Table 3 presents teleseismic P m_b data determined by Stevens (1980) for the Sharpsburg earthquake. Assuming a t^* of 1.0 and calculating synthetic P seismograms yields an average m_b of only 3.9

compared to the observed 4.8. This is complicated by an amplitude instability due to the strike-slip source model. Several stations in western Canada lie near the theoretical P wave node for the choice of orientation used (dip, 50°; slip, 180°; strike, 30°) for the synthetics. Since the orientation is only known to within about $\pm 10^\circ$ for all angles, synthetic amplitudes for these stations will display large variations for small changes in the fault orientation. An average m_b of only 4.1 is calculated disregarding these nodal stations, still too low by nearly an order of magnitude. Assuming a t^* of 0.5 dramatically improved the m_b comparison. Scaling the t^* at NORSAR to yield the correct observed P amplitude for a moment of 4×10^{23} dyne-cm yields a t^* of 0.7.

These t^* calculations are subject to many unknowns, particularly those due to uncertainties in geometric spreading, the uncertainties in the surface wave seismic moment calculation, and possible uncertainties in the shape of time function. Values of t^* lower than 1.0 at 1 second period are consistent with other estimates of teleseismic t^* for non-tectonic areas (e.g. Frasier and Filson, 1972), although there is continuing debate on this topic (Helmberger and Hadley, 1981; Der and McElfresh, 1980). The t^* values determined here need further independent confirmation before being accepted.

AFTERSHOCK STUDIES

Aftershocks of the July 27, 1980 Sharpsburg, Kentucky earthquake were monitored with portable instruments by groups from the University of Michigan, the University of Kentucky, Virginia Polytechnic Institute and State University, the Tennessee Earthquake Information Center, and the U.S. Geological Survey. Saint Louis University participated by loaning the UK/TEIC party six sets of instruments. 31 sets of portable instruments were available, mainly analog smoked-paper or pen-and-ink systems recording only the vertical component of

ground motion. Five three-component triggered-digital seismographs were deployed by the USGS. 48 recording sites were occupied during the field program. Figure 7 shows the locations of the recording sites.

Monitoring was begun by a team from the University of Michigan about 15 hours after the main shock, at a site about 45 km from the main shock epicenter. The TEIC/UK group began monitoring within 5 km of the main shock about 17.5 hours after it occurred. By 2300Z on July 29, seven stations were operating at distances of 4-23 km from the aftershock zone. While the UM team pulled out late on July 30, the arrival of the USGS and VPI groups and the installation of additional stations by the UK/TEIC rapidly improved the coverage. Some initial confusion about the main shock epicenter was caused by the apparent high-intensities observed at Maysville, Kentucky, (Figure 7) about 50 km north of Sharpsburg (Reagor *et al*, 1981). Initially a number of stations were deployed in this general area. However, by July 30, epicenters had been obtained for one or two aftershocks and the USGS and VPI groups relocated. On August 1 at least 15 stations were operating within 30 km of the aftershock zone. Such dense monitoring continued until August 8-10, when waning activity caused all groups to either pull out or reduce the number of monitoring sites. Nearly continuous recording has been maintained in the area by one to two semi-permanent stations installed by the UK and the TEIC. Station location and operational information are contained in Table 4.

Figure 8 plots the rate of occurrence of aftershocks with respect to time. Aftershock activity was light for an earthquake of this magnitude. In spite of the early installation of high-gain instruments very close to the epicenter, only 69 aftershocks have been identified through early May 1981. Nearly half of the identified aftershocks occurred within 96 hours of the main quake; the occurrence rate dropped dramatically after the largest felt aftershock occurred

on July 31. Only 16 aftershocks exceeded magnitude $M_L = 0$, and the largest aftershock had a magnitude of only $m_{bLg} = 2.2$. Two events in the magnitude 1.5 range occurred before the installation of any temporary stations. These aftershocks were identified on records of the TEIC station in Tuckaleechee Caverns, Tennessee (TKL), at a distance of about 280 km from Sharpsburg. Presumably a number of smaller aftershocks also occurred in this time interval. The aftershock list presented in Table 5 is probably complete down to magnitude $M_L = -1$ after about 1800Z on July 28. Magnitudes were computed down from formulae for M_L (duration) (Bollinger *et al.*, 1976) and m_{bLg} (Nuttli, 1973). They were found to be roughly equivalent in the range 0.4 to 2.2 when both types of magnitude could be computed, and so are used interchangeably.

Several aftershocks were felt. That of July 31, 1980 (magnitude 2.2) awakened sleepers over an area of several hundred square km and did additional damage to a house south of Sharpsburg that had been badly damaged in the main shock. The earthquakes of August 25 (magnitude 2.0) and December 30 (magnitude 1.6) were felt over areas of roughly 500 to 1000 square km, respectively. Earthquakes on July 30, 1980 and January 14, 1981, both of magnitude 1.5, were reported felt by a few persons in the Sharpsburg area. A magnitude 0.7 quake on February 6, was also reported felt, but this is considered doubtful.

It is unusual for such small events to be felt over such large areas. For example, Nuttli and Zollweg (1974) found that central United States earthquakes with felt areas of 500 to 1000 square km generally had magnitudes in the range of 3 to 3.5, while earthquakes in the magnitude interval of 1.5 to 2.2 normally were not felt at all. This effect can only partly be explained by the idea of a "sensitized population" noticing smaller shocks than they normally would. The July 31 earthquake occurred in the early morning when many were asleep, yet was the most widely perceived aftershock.

Data Analysis.

Arrival times of aftershock phases were read to the nearest 0.05 or 0.1 second, depending on whether the drum speed of the original record was 120 or 60 mm/min, respectively. Somewhat higher resolution of the arrival times is possible by enlarging the original records, but the sheer number of stations that were available for most events makes it highly unlikely that the conclusions of this study would be seriously altered, although it is possible that smaller standard errors in the locations could result. In general, P- and S-wave arrivals were sharp and clear on most stations, although a few seem to have been near nodes of the SV-wave radiation pattern. Since no horizontal-component information was available, all readings for S were made from vertical seismographs.

To mitigate potential timing problems due to inaccurate drum rotation, nearly all stations superimposed either 1-second or 10-second time marks on the data. With the exception of two instruments, chronometer drift rates were less than about 0.1 second per day. All readings were made by the same analyst, and were subjectively weighted according to quality on a scale ranging from 0 (highest quality) to 4 (not used).

Brumfield (1982) used data generated by a number of limestone quarries exist in the region of the station network to establish a local velocity model. Two of the quarries, at Flemingsburg and North Middletown, were so situated that a line through them passed along the northwest edge of the aftershock region. This suggested construction of a reversed refraction profile, since most stations recorded at least one blast from each area. Brumfield (1982) found a velocity of 6.87 km/sec for P-waves refracted at a depth of about 0.8 km and 3.91 km/sec for the corresponding S-wave. Dip along the reversed profile was negligible. Several more distant quarry blasts ($\Delta \geq 100$ km) were also examined. P-wave phase velocities across the network ranged roughly between $6 \frac{3}{4}$ and 7

km/sec, confirming the result from local blasts and indicating there is little if any dip at right angles to the reversed profile. A P-wave velocity of 5.52 km/sec was used for the top 1 km of sedimentary rocks; this was the average of several well velocities provided by an oil company that had drilled in the area.

These velocities are unexpectedly high for such shallow depths. They are roughly equivalent to some surface velocities in New England and the Canadian Shield where the paths are entirely through highly-competent metamorphic and igneous material. The *Basement Rock Map of the United States* (Bagley and Muehlburger, 1968) indicates that the epicentral region lies just a few km south of the maximum extent of the Grenville Front, and that the hypocentral region would be in the Grenville Province if it extended farther south. Aside from these considerations, the P- and S-wave data sets for 29 of the best-recorded aftershocks were run independently using HYPO71 (Lee and Lahr, 1971). While the epicenters agreed for the two independent sets with almost any reasonable choice of velocities (this is because very little data were available for distances greater than 25 km), velocities similar to those found in the refraction experiment were required to get the focal depths to agree.

No good information is presently available on the deeper velocity structure. Since the velocity at a depth of only 1 km exceeds that assigned by Nuttli *et al.*, (1969) for depths of between 20 and 40 km in the Central United States, it is presently hypothesized that the 8.85 km/sec velocity for P waves can be applied as far down as the Moho, or to a depth of around 40 km. The velocity model, based on the work of Brumfield (1982), used to locate the aftershocks is given in Table 6.

Because the network used to record the Sharpsburg aftershocks varied on practically a day-to-day basis, joint-hypocenter determination techniques were used to locate the better-recorded events relative to a particularly well-

recorded aftershock (Herrmann *et al.*, 1981). 52 earthquakes recorded by a minimum of three stations observing both P and S were chosen. The reference event used was the aftershock at 0812Z on August 3. Its HYP071 location was assumed to be fixed.

Relative locations in general were quite good, with most having horizontal and vertical error-ellipse major-axes less than 0.8 km for 95% confidence. Figure 9 shows that there is no distinct trend in the epicenters, which cluster in an area of about 30 square km. However, vertical profiles plotted at various azimuths clearly show the aftershock zone dipping at about 50 degrees to the southeast (Figure 9). The strike corresponding to this dip is about N30E, with an error not exceeding ten degrees. The fault area involved is about 30-50 square km.

Individual fault plane solutions could be determined for only two aftershocks: that of 1701Z July 30, 1980 (magnitude 1.5) and that of 0926Z July 31, 1980 (magnitude 2.2). While the solutions differ in the nature of the faulting indicated, a plane striking NNE is common to both. Figure 10 shows that the 30 July shock was nearly pure thrust, while the July 31 earthquake had a strike-slip mechanism very similar to that of the main shock. A composite solution (Figure 10) for the remaining events is very similar to the solution for the July 27 main shock. From these solutions, it is estimated that the preferred fault plane strikes about N20-30E and dips 50 degrees to the southeast, in very close agreement with the strike and dip of the aftershock zone.

Discussion

The importance of the aftershock study lies not in any innovation of technique or instrumentation, but rather in the fact that it is the first time that an aftershock sequence of a moderate eastern North American earthquake has been adequately observed. The exceptionally rapid deployment of portable

instruments was the major departure from previous studies such as those of Lange and Westphal (1963), Stauder and Pitt (1970), or Bollinger *et al.*, (1976), wherein the temporary networks were not operational for at least two to three days after the main shocks. In addition, the large number of instruments used in the present study allowed some margin for error, i.e., virtually the entire meizoseismal area was instrumented and therefore the location of the main shock was not as critical as it might have been if, for example, only five or six portable seismographs been available. The rapid decrease of activity following the large aftershock of July 31 confirms the importance of installing temporary stations as soon as possible after the main shock, if significant results are to be obtained.

For so large an earthquake, both the total number of aftershocks and the maximum magnitude aftershock are anomalous. Such weak aftershock sequences, however, seem to be typical of many eastern North American earthquakes. If the Sharpsburg sequence is considered to be normal, insofar as eastern earthquakes are concerned, the failure of previous investigations to record aftershocks for similarly large events in the last two decades is readily explained.

Apart from the small number of events involved and the low overall energy release of the total aftershock sequence, there does not seem to be anything particularly unusual about Sharpsburg aftershocks. The clustering of the aftershocks about a planar surface allows for the first time an independent estimate of the source area of an eastern earthquake of moderate size. The length of this zone along the strike is 6 to 7 km. This observed result clearly refutes the suggestion of Evernden (1975) that eastern United States earthquakes have much smaller fault lengths when compared to western earthquakes of the same magnitude. Table 7 and Figure 11 compare the maximum length of the

Sharpsburg aftershock zone with several western United States earthquakes for which detailed aftershock investigations were made. It is clear that the Sharpsburg fault length falls well within the range, although near its lower end. This plot ignores the possibility that there is a bias in teleseismic m_b between eastern and western U. S. earthquakes. Herrmann and Nuttli (1982) presented evidence that the western m_b is about 0.4 units lower than that of an equivalent eastern U. S. earthquake. Equalizing for this magnitude bias would lower the Sharpsburg m_b or raise the other m_b 's by 0.4 magnitude units. but would not alter the conclusion that the Sharpsburg fault length is within the range for earthquakes of similar magnitude.

Given a seismic moment $M_o = 4.1 \times 10^{23}$ dyne-cm for the main shock and assuming that the aftershock zone corresponds to the fault surface of the main shock, estimates of the dislocation and stress drop of the main shock can be made. Assuming $\mu = 4 \times 10^{11}$ dyne/cm² and a fault area of 30 - 50 km², the average dislocation \bar{u} is obtained from

$$M_o = \mu \bar{u} A$$

from which we estimate $\bar{u} = 2 - 3.4$ cm. Using a relation for the stress drop for an instantaneous dislocation on a circular fault plane, (Brune, 1970),

$$\Delta\sigma = \frac{7}{16} \frac{M_o}{r^3}$$

we find $\Delta\sigma = 2.8 - 6$ bars by using $r = 3.1 - 4.0$ km. Assuming that the frequency content of the far-field P pulse is the same as that of the S pulse for a small earthquake of this size, we can estimate the corner frequency $f_o = 2.34 \beta / 2\pi r = 0.36 - 0.36$ Hz using the equivalent radius r (Brune, 1970). A triangular source time function with total duration of 1.0 sec would have a corner frequency between 0.6-0.9 Hz. Thus the aftershock fault dimension, r , is consistent with the duration of the P wave pulse obtained from the NORSAR data.

CONCLUSIONS

The Sharpsburg, Kentucky earthquake is now one of the best studied eastern North American earthquakes. On the basis of the seismic moment, it is the second largest earthquake to have occurred in eastern North America since 1961 (Herrmann, 1979), second only to the November 9, 1968 southern Illinois earthquake. The focal mechanism was constrained by two independent data sets. The focal depth of the main shock was constrained by surface wave spectral amplitude data, teleseismic P-waveforms and aftershock locations. A focal depth of 12 km is reasonable. The seismic moment, magnitude and stress drop are consistent with other eastern U.S. earthquakes studied (Street *et al.*, 1975; Street and Turcotte, 1977). Even though the seismic source parameters are within the range of expected values, the question of why the earthquake occurred when it did cannot be answered from the present data.

This study routinely used recently developed seismic waveform modeling techniques. In the case of the regional waveforms, more data would have been available if long period analog seismograms had not been saturated. If we are to obtain the maximum information from such earthquakes in the future, the instrumentation will have to be improved to match our computational abilities.

ACKNOWLEDGMENTS

We are particularly indebted to Ron Street of the University of Kentucky and his students for coordinating and performing much of the aftershock study. Doug Christensen, Gil Bollinger, and Charley Langer made available the original seismograms recorded by aftershock study groups from the University of Michigan, Virginia Polytechnic Institute and State University, and the U.S. Geological Survey, respectively. Mr. Ray Robertson of Bethel, Kentucky has continued to operate the BETH station to provide ongoing monitoring of late aftershocks. We

are grateful to the numerous landowners who allowed operation of the temporary stations on their property.

We would like to thank Dr. E. Husebye for providing a copy of the NORSAR data. This research was supported by the Advanced Research Projects Agency of the Department of the Defense and was monitored by the Air Force Office of Scientific Research under Grant AFOSR-78-3528 (CAL), the U. S. Nuclear Regulatory Commission under Contract NRC-04-76-282 and the U. S. Geological Survey under Contracts 14-08-0001-16708 and 14-08-0001-19751 (RBH), the U. S. Nuclear Regulatory Commission under Contracts NRC-04-78-200 and NRC-04-79-214 and by the State of Tennessee (JEZ).

REFERENCES

- Allison, M.L., J.H. Whitcomb, C.E. Cheatum, and R.B. McKuen (1978). Elsinore fault seismicity: the September 13, 1973, Agua Caliente Springs, California earthquake sequence, *Bull. Seism. Soc. Am.* 68, 429-440.
- Bagley, R.W. and W.R. Muehlburger (1968), compilers, *Basement Rock Map of the United States*, U.S. Geological Survey.
- Bollinger, G.A., C.J. Langer, and S.T. Harding (1976). The eastern Tennessee earthquake sequence of October through December, 1973, *Bull. Seism. Soc. Am.* 66, 525-548.
- Brumfield, K. (1982). A geophysical investigation of the Paleozoic sedimentary sequence in the Precambrian basement structure in the Sharpsburg, Kentucky area, *M.S. Thesis*, University of Kentucky, Lexington, Ky.
- Brune, J.N. (1970). Tectonic stress and the spectra of seismic shear waves from earthquakes, *J. Geophys. Res.* 75, 4997-5009.
- Der, Z.A. and T.W. McElfresh (1980). On the value of t_p^* and t_s^* in the short-period band and regional variations of the same across the United States, *Bull. Seism. Soc. Am.* 70, 921-924.
- Dziewonski, A., S. Block and M. Landisman (1969). A technique for the analysis of transient seismic signals, *Bull. Seism. Soc. Am.* 59, 427-444.
- Eaton, J.P., M.E. O'Neill, and J.N. Murdock (1970). Aftershocks of the 1965 Parkfield-Cholame, California, earthquake: a detailed study, *Bull. Seism. Soc. Am.* 60, 1151-1197.
- Ellsworth, W.L. (1975). Bear Valley, California, earthquake sequence of February-March 1972, *Bull. Seism. Soc. Am.* 65, 483-506.

- Evernden, J.F. (1975). Seismic intensities, "size" of earthquakes and related parameters, *Bull. Seism. Soc. Am.* 65, 1287-1314.
- Frasier, C. and J. Filson (1972). A direct measurement of the earth's short-period attenuation along a teleseismic ray path, *J. Geophys. Res.* 77, 3782-3791.
- Futterman, W.I. (1962). Dispersive body waves, *J. Geophys. Res.* 67, 5279-5291.
- Grant, W.C., C.S. Weaver, and J.E. Zollweg (1981). The February 14, 1981, Elk Lake, Washington, earthquake and its aftershock sequence (abstract), *EOS* 62, 966.
- Helmberger, D.V. and D.M. Hadley (1981). Seismic source functions and attenuation from local and teleseismic observations of the NTS events Jorum and Handley, *Bull. Seism. Soc. Am.* 71, 51-68.
- Herrmann, R.B. (1979). Surface wave focal mechanisms for eastern North American earthquakes with tectonic implications, *J. Geophys. Res.* 84, 3543-3552.
- Herrmann, R. B. (1981). Waveform studies of the July 27, 1980 Kentucky earthquake (abstract), *Earthquake Notes* 52, 33.
- Herrmann, R.B. and B.J. Mitchell (1975). Statistical analysis and interpretation of surface-wave anelastic attenuation data for the stable interior of North America, *Bull. Seism. Soc. Am.* 65, 209-218.
- Herrmann, R.B., J.W. Dewey and S.K. Park (1980). The Dulce, New Mexico, Earthquake of 23 January 1966, *Bull. Seism. Soc. Am.* 70, 2171-2184.
- Herrmann, R.B., S.K. Park and C.Y. Wang (1981). The Denver Earthquakes of 1967-1968, *Bull. Seism. Soc. Am.* 71, 731-746.
- Herrmann, R. B. and O. W. Nuttli (1982). Magnitude: the relation of M_L to m_{BL} , *Bull. Seism. Soc. Am.* 72, 389-397.

- Lange, A.L., and W.H. Westphal (1963). Seismic aftershock investigations - Project VELA UNIFORM, Fisk, Missouri, earthquake of 3 March 1963, *Technical Report No. 3 prepared for Advanced Research Projects Agency by Stanford Research Institute under Contract AF 49(638)-1205*.
- Langston, C.A. (1981). Source inversion of seismic waveforms: The Koyna, India, earthquakes of 13 September 1967, *Bull. Seism. Soc. Am.* 71, 1-24.
- Langston, C.A. and D.V. Helmberger (1975). A procedure for modeling shallow dislocation sources, *Geophys. J.* 42, 117-130.
- Lee, W.H.K., and J.C. Lahr (1975). HYP071 (Revised): a computer program for determining hypocenter, magnitude, and first motion pattern of local earthquakes, *U.S. Geol. Surv., Open-File Rept. 75-311*, 113 pp.
- Mauk, F. J. and D. H. Christensen (1980). The Sharpsburg, Kentucky, earthquake of 27 July 1980: main shock mechanism and isoseismal data (abstract), *Earthquake Notes* 51, 26.
- Mauk, F. J., D. Christensen, and S. Henry (1982): The Sharpsburg, Kentucky earthquake of 27 July 1980: main shock parameters and isoseismal maps, *Bull. Seism. Soc. Am.* 72, 000-000.
- Mohler, A.S. (1980). Earthquake/earth tide correlation and other features of the Susanville, California, earthquake sequence of June-July 1976, *Bull. Seism. Soc. Am.* 70, 1583-1593.
- Morrison, P.W., Jr., B.W. Stump, and R. Uhrhammer (1976). The Oroville earthquake sequence of August 1975, *Bull. Seism. Soc. Am.* 66, 1065-1084.
- Nuttli, O.W. (1973). Seismic wave attenuation and magnitude relations for eastern North America, *J. Geophys. Res.* 78, 876-885.
- Nuttli, O.W., and J.E. Zollweg (1974). The relation between felt area and magnitude for Central United States earthquakes, *Bull. Seism. Soc. Am.* 64, 73-86.

- Nuttli, O.W., W. Stauder, and C. Kisslinger (1969). Travel time tables for earthquakes in the central United States, *Earthquake Notes* 40, 19-28.
- Pearce, R.G. (1977). Fault plane solutions using relative amplitudes of P and pP, *Geophys. J.* 50, 381-394.
- Reagor, B.G., C.W. Stover, and M.G. Hopper (1981). Preliminary report of the distribution of intensities for the Kentucky earthquake of July 27, 1980, U.S. Geol. Surv., *Open-File Rept. 81-198*, 71 pp.
- Somerville, M.R., W.A. Peppin, and J.D. Van Wormer (1980). An earthquake sequence in the Sierra Nevada - Great Basin boundary zone: Diamond Valley, *Bull. Seism. Soc. Am.* 70, 1547-1555.
- Stauder, W., and A.M. Pitt (1970). Note on an aftershock study, South Central Illinois earthquake of November 9, 1968, *Bull. Seism. Soc. Am.* 60, 983-986.
- Stevens, A.E. (1980). Canadian magnitude determinations for the Sharpsburg, Northern Kentucky, earthquake of 27 July 1980, Seismological Service of Canada Internal Report 80-11, Division of Seismology and Geothermal Studies, Earth Physics Branch, Dept. of Energy, Mines and Resources, Ottawa, Canada.
- Stierman, D.J., and W.L. Ellsworth (1976). Aftershocks of the February 21, 1973 Point Mugu, California earthquake, *Bull. Seism. Soc. Am.* 66, 1931-1952.
- Street, R.L., R.B. Herrmann and O.W. Nuttli (1975). Spectral characteristics of the Lg wave generated by central United States earthquakes, *Geophys. J.* 41, 51-63.
- Street, R.L. and F.T. Turcotte (1977). A study of northeastern North American spectral moments, magnitudes and intensities, *Bull. Seism. Soc. Am.* 67, 599-614.

Thatcher, W., and R.M. Hamilton (1973). Aftershocks and source characteristics of the 1969 Coyote Mountain earthquake, San Jacinto fault zone, California *Bull. Seism. Soc. Am.* **63**, 647-662.

Wu, F.T. (1968). Parkfield earthquake of June 28, 1966: magnitude and source mechanism, *Bull. Seism. Soc. Am.* **58**, 689-710.

Zollweg, J.E., and R.S. Crosson (1981). The Goat Rocks Wilderness, Washington, earthquake of 28 May 1981 (abstract), *EOS* **62**, 966.

Department of Earth and Atmospheric Sciences
Saint Louis University
P.O. Box 8099
St. Louis, MO 63156 (RBH)

Department of Geosciences
The Pennsylvania State University
403 Deike Building
University Park, PA 16802 (CAL)

Tennessee Earthquake Information Center
Memphis State University
Memphis, TN 38152 (JEZ)

FIGURE CAPTIONS

Figure 1. The nodal planes satisfy surface-wave spectral amplitude data as well as P-wave first motion data. Circles and triangles indicate compressional and dilatational first motion, respectively. The symbols T and P are intersections of the tension and pressure axes, respectively, with the lower hemisphere. An equal area lower hemisphere projection is used. Only sharp, impulsive first motion data are used. The northeast nodal plane strikes 30° , dips 60° and has a slip angle of 180° .

Figure 2. Comparison between anelastic attenuation corrected, observed and predicted Love-wave and Rayleigh-wave radiation patterns at selected periods T. The scaling bars are spectral amplitudes in units of cm-sec at a reference distance of 9° from the source.

Figure 3. Observed and predicted long period vertical seismograms at SLM, a distance of 555 km from the earthquake. 128 seconds of time history are plotted starting 90 seconds after the origin time. The number by each trace is the zero-to-peak amplitude in cm on a 15-100 WWSSN long period seismogram with peak magnification of 3000. Predicted traces are for depths of 11, 15 and 20 km in the Central U. S. earth model.

Figure 4. Observed and predicted long period three component seismograms at HLA, a distance of 326 km from the earthquake. 128 seconds of time history are plotted, with traces starting 40.2 seconds after the origin time. The number by each trace is the zero-to-peak amplitude in cm on a 15-100 WWSSN long period seismogram with peak magnification of 3000. The central U. S. model was used for depths of 11, 15 and 20 km while the Appalachian Basin model was used for the focal depth of 14 km.

Figure 5. Observed (top) P waveform at NORSAR with synthetic waveforms (below). Crustal model, dip, strike and rake angles are given for each synthetic. Zero-to-peak amplitude for the observed trace is in quantized units (Q. U.). For NORSAR sensors, there are 0.0427 nm/ Q. U. at 1.0 Hz.

Figure 6. Acceptable fault plane solutions for the body wave data from the Sharpsburg earthquake under various assumptions concerning the input data. P nodal planes are shown on an equal area projection of the lower focal hemisphere. All solutions are right-lateral on the NE trending planes. All possible solutions were tested with an increment angle of 5° in strike, dip, and slip.

Figure 7. Locations of portable seismograph stations deployed for the aftershock study. The station coordinates are given in Table 4. The locations of Maysville and Sharpsburg, Kentucky are indicated.

Figure 8. Plot of aftershock activity rate through August 25, 1980.

Figure 9. Hypocenter locations after using relocation techniques. Epicenters and two vertical depth profiles are shown. The seismograph stations are indicated by triangles with their names given on the base map. There is no vertical exaggeration on the depth profiles. Profile AB strikes $N30^\circ E$ and profile CD strikes $N120^\circ E$.

Figure 10. Lower hemisphere, equal-area projections of focal mechanism solutions for two well recorded Sharpsburg aftershocks, and a composite solution for the remaining better located aftershocks. Solid circles and triangles indicate sharp compressional and dilatational first arrivals, respectively. Open symbols denote poorer quality but clear first arrivals. Nodal quality arrivals are denoted by an X.

Figure 11. Plot of teleseismic m_b versus fault length for earthquakes listed in Table 7. The open symbols are western events and the solid symbol is the Sharpsburg event.

Table 1

Earth Models

	Thickness (km)	V_p (km/sec)	V_s (km/sec)	ρ (gm/cm ³)	Q_α	Q_β
Central U.S.						
	1	5.0	2.89	2.5	4000	2000
	9	6.10	3.52	2.7	4000	2000
	10	6.40	3.70	2.9	4000	2000
	20	6.70	3.87	3.0	4000	2000
	—	8.15	4.70	3.4	4000	2000
Appalachian Basin						
	3	5.00	2.89	2.5	4000	2000
	9	6.10	3.52	2.7	4000	2000
	10	6.40	3.70	2.9	4000	2000
	20	6.70	3.87	3.0	4000	2000
	—	8.15	4.70	3.4	4000	2000

Table 2

Crustal Models used in the Body Wave Analysis

	V_p (km/sec)	V_s (km/sec)	ρ (gm/cm ³)	Th(km)
MODEL A	6.0	3.5	2.7	14.
	6.7	3.9	2.9	20.
	8.1	4.7	3.2	-
MODEL B	6.7	3.9	2.9	-
MODEL C	5.6	3.0	2.6	2.0
	6.0	3.5	2.7	12.0
	6.7	3.9	2.9	20.0
	8.1	4.7	3.2	-

Table 3

Canadian Network m_b

Station	$\Delta^{(e)}$	AZ ^(e)	m_b Observed ¹	m_b Calc. $t^*=1.0$	m_b Calc. $t^*=0.5$
PIB(N)	30.2	303	4.88	3.3	4.0
PGC(N)	30.3	303	4.64	3.3	4.0
YKC	30.7	332	4.82	4.3	5.0
ALB	31.2	304	4.74	3.4	4.1
IGL	31.3	2	5.31	4.4	5.1
FSB	31.8	314	4.57	4.0	4.6
GDR(N)	32.1	305	4.68	3.5	4.2
PHC(N)	33.1	307	5.25	3.6	4.3
RES	37.0	355	4.59	4.4	4.8
WHC	38.9	322	4.13	3.9	4.5
INK	40.4	334	4.62	4.0	4.7
KEY	40.6	323	4.46	3.9	4.5
MBC	41.3	348	5.27	4.1	4.8
KRY	41.6	325	4.71	3.9	4.6
ALE	45.1	4	5.25	4.3	5.0
average			4.8±0.3	3.9± 0.4	4.5±0.4
average excluding nodal stations (N)			4.8±0.4	4.1±0.2	4.8 ±0.2

1 from Stevens (1980)

Table 4. Station Coordinates

Station Name	Other Name	Lat (°N)	Lon (°W)	Elev (m)	Group	Place
BEKY	BCM	38.254	83.861	280	USGS	Bethel-Longview Cemetery
BETH		38.247	83.853	278	UK/TEIC	Bethel
CARL	CCM	38.320	84.034	271	USGS	Carlisle
CLAY		38.197	83.910	302	UK/TEIC	Sharpsburg-Clay Site 1
CMG	UMO	37.993	83.864		UM	Camargo
CTOH	CLY	38.747	83.872		USGS	Clayton, Ohio
ELZ		38.385	83.800	288	VPI&SU	Elizaville
FAIR	CEM	38.458	83.938	277	USGS	Fairview
FROG	WES2	38.287	83.979	307	UK/TEIC	Frogtown (Weston Site 2)
GSA		38.297	83.623	276	VPI&SU	Girl Scout Camp
JUDY		38.137	83.948	293	UK/TEIC	Judy
LEV		37.981	83.966	250	USGS	Levee
MHK	UM3A	38.568	83.866		UM	Murphysville Bridge
MGS	MAY	38.593	83.848	264	USGS	Murphysville-GS
MOK	UM1	38.582	84.064		UM	Mount Olivet
MSGS	MTS	38.031	83.924	293	USGS	Mt. Sterling-GS
MSK		38.038	83.915	298	UK/TEIC	Mt. Sterling
MUR	UM3B	38.577	83.864		UM	Murphysville
NMK	NMC	38.143	84.092	291	USGS	North Middletown
ODD	UM2A	38.462	84.239		UM	Oddsville
ODD2	UM2B	38.467	84.238		UM	Oddsville Site 2
OSKY	OLS	38.055	83.849	241	VPI&SU	Olympia Springs
OWG		38.173	83.825	304	UK/TEIC	Owingsville
PLJM		38.168	84.073	282	UK/TEIC	Plum
PRR		38.089	84.161	288	USGS	Pretty Run Road
REY		38.220	83.848	262	UK/TEIC	Reynoldsville
RMK	RUD	38.299	84.241	262	USGS	Ruddels Mills
SCF	CLAY	38.198	83.909	300	UK/TEIC	Sharpsburg-Clay Farm 1
SGS	7SR	38.191	83.932	280	USGS	Sharpsburg-GS
SHER		38.284	83.837	272	UK/TEIC	Sherburne
SNR	SBK	38.179	83.958	294	UK/TEIC	Sharpsburg-Nixon Road
SPKY	STC	38.125	84.210	271	USGS	Stony Point
SSA	CRO	38.225	83.928		UK/TEIC	Sharpsburg-Sunny Acres
TKL		35.858	83.774			
WASH	WSH	38.604	83.800	267	VPI&SU	Washington
WES		38.287	83.976	311	UK/TEIC	Weston Site 1

Table 5. Aftershock Locations

Date	Time	Lat (°N)	Lon (°W)	Depth (km)	ERH (km)	ERZ (km)	M _L	mbl _g
27 JUL 80	20 58 08							1.5
27 JUL 80	22 58 05							1.2
28 JUL 80	10 39 45.5							1.2
28 JUL 80	10 59 08.9						(0.5)	
28 JUL 80	11 32 47.1						(0.5)	
28 JUL 80	14 15 58.2	38.192	83.971	1.0	2.0	11.9	-0.3	
28 JUL 80	15 25 7.4	38.213	83.990	7.7	2.0	1.0	-0.5	
28 JUL 80	17 25 36						-0.8	
28 JUL 80	20 13 29.3	38.236	83.871	1.2	1.6	11.9	-0.8	
29 JUL 80	4 1 53.3	38.188	83.930	11.5	.9	1.3	0.8	0.4
29 JUL 80	4 9 5.6	38.194	83.908	12.2	1.0	1.4	-0.8	
29 JUL 80	6 18 1.8	38.193	83.913	13.7	1.2	1.3	-0.6	
29 JUL 80	07 59 23						(-1.0)	
29 JUL 80	7 59 37.8	38.177	83.937	10.3	1.1	1.8	-0.5	
29 JUL 80	12 55 32.9	38.175	83.938	11.2	1.2	1.6	-0.2	
29 JUL 80	18 8 26.6	38.177	83.962	2.0	.8	.9	-0.6	
29 JUL 80	20 52 21.3	38.189	83.921	11.8	2.0	1.8	-0.8	
29 JUL 80	21 12 24.7	38.199	83.939	10.7	1.8	1.8	-0.8	
29 JUL 80	22 4 23.7	38.200	83.902	13.1	2.0	1.3	-0.6	
30 JUL 80	4 52 27.0	38.226	83.949	6.2	.8	1.4	-1.1	
30 JUL 80	8 0 56.5	38.197	83.941	11.0	.9	.9	-0.8	
30 JUL 80	7 9 59.4	38.181	83.948	8.8	.8	2.2	-1.3	
30 JUL 80	8 31 55.8	38.174	83.938	9.0	.5	.9	-0.3	
30 JUL 80	9 31 17.8	38.219	83.902	6.5	.6	1.4	-0.8	
30 JUL 80	9 31 44.3	38.217	83.902	6.2	.5	1.3	-0.8	
30 JUL 80	10 0 59.1	38.192	83.933	10.5	1.0	1.3	-0.9	
30 JUL 80	12 39 21.1	38.206	83.935	9.0	.7	1.2	-0.8	
30 JUL 80	16 29 52.0	38.178	83.939	10.7	.8	1.2	-0.8	
30 JUL 80	17 0 34.4	38.196	83.918	9.6	.6	.8	-0.8	
30 JUL 80	17 1 41.2	38.190	83.920	11.4	.6	.7	1.5	1.3
Felt at Sharpsburg. MMI II.								
30 JUL 80	18 40 11.9	38.193	83.917	11.6	.6	.7	-0.1	
31 JUL 80	0 48 53.5	38.183	83.926	11.4	.5	.8	-1.1	
31 JUL 80	0 53 42						-1.3	
31 JUL 80	1 49 27.4	38.190	83.928	12.5	.8	.8	-1.2	
31 JUL 80	2 41 57.8	38.194	83.923	13.4	.8	1.1	-1.2	
31 JUL 80	7 23 34.8	38.185	83.928	11.5	.6	.7	-0.9	
31 JUL 80	9 28 56.9	38.193	83.930	10.8	.5	.9	1.9	2.2
Felt widely. MMI IV at Sharpsburg.								
Some additional damage to house south of Sharpsburg damaged by the main shock.								
31 JUL 80	9 31 48.8	38.204	83.960	8.8	1.5	1.9	-1.2	
31 JUL 80	9 36 34.4	38.201	83.941	9.9	.9	1.0	-1.0	
31 JUL 80	18 57 58.3	38.181	83.919	11.8	.8	.7	-0.1	
31 JUL 80	22 5 57.8	38.176	83.938	11.5	.8	.8	-1.1	
31 JUL 80	23 28 3.8	38.171	83.928	12.0	.6	.6	-0.6	
1 AUG 80	23 36 18						-1.5	
2 AUG 80	1 23 14.4	38.174	83.921	12.8	.8	.6	-1.5	
2 AUG 80	7 58 10.5	38.179	83.931	12.2	.9	.9	-1.1	
2 AUG 80	18 28 33.2	38.186	83.929	10.9	.5	.5	-0.3	
3 AUG 80	8 12 20.4	38.181	83.917	12.2	.3	.4	0.4	0.1
3 AUG 80	8 34 52.4	38.199	83.924	10.8	.4	.5	-0.7	
3 AUG 80	21 42 7.0	38.184	83.937	11.4	.5	.6	-0.7	
4 AUG 80	2 14 33.9	38.193	83.921	10.3	.8	.6	-0.6	
4 AUG 80	3 57 58.8	38.179	83.932	11.8	.8	.6	-0.9	
5 AUG 80	18 24 43.0	38.198	83.922	11.0	.5	.6	0.2	
7 AUG 80	14 18 56.0	38.181	83.948	11.8	.5	.6	-0.6	
8 AUG 80	0 21 11.0	38.180	83.909	12.2	.6	.6	-0.8	
8 AUG 80	2 0 56.8	38.176	83.937	11.0	.5	.6	-0.2	
8 AUG 80	4 52 29.2	38.191	83.929	10.5	.5	.6	-0.1	

10	AUG	80	19	3	18.7	38.183	83.933	10.3	3.2	1.0	-0.8	
10	AUG	80	19	24	29.4	38.193	83.894	10.8	3.2	1.4	-0.8	
11	AUG	80	18	3	54.4	38.182	83.939	10.1	3.1	1.2	0.4	
11	AUG	80	18	51	41.9						-0.5	
16	AUG	80	21	42	36.8						-0.3	
21	AUG	80	18	15	13.9						-0.8	
25	AUG	80	11	41	37.7	38.20	83.92	1.0	.6	.3	1.7	2.0
Felt at Bethel, Sherburne and Sharpsburg												
Maximum intensity MMI IV near Sherburne												
29	SEP	80	17	14	58.5						1.2	
30	DEC	80	03	07	08						1.8	
Felt in portions of four counties.												
Maximum intensity MMI IV near Sharpsburg.												
14	JAN	81	21	10	14						1.5	
Felt by some in vicinity of Sharpsburg.												
23	JAN	81	04	55	03						-0.2	
29	JAN	81	05	38	21						-0.2	
06	FEB	81	10	32	38						0.7	

Notes:

1. M_L obtained using relation from Bollinger *et al* (1976).
2. m_{bLg} determinations are from TKL seismograms, except for 31 JUL 1980 0926UT for which TKL and PWLA were used.

Table 8

Velocity Model used to Locate Sharpsburg Aftershocks

<u>Layer Thickness (km)</u>	<u>Depth to Top (km)</u>	<u>V_p(km/sec)</u>	<u>V_s(km/sec)</u>
1.0	0.0	5.52	3.15
39.0	1.0	6.85	3.91

Table 7
Comparison of Aftershock Zone Lengths

Date	m_b	M_s	M_L	L(km)	Location	Reference
1968 28 JUN	5.8	6.4	5.5	40	Parkfield, CA	1,2
1969 28 APR	5.7	5.2	5.8	35	Coyote Mtn., CA	3
1972 24 FEB	4.9	4.0	5.0	8.5	Bear Valley, CA	4
1973 21 FEB	5.7	5.2	6.0	10	Pt. Mugu, CA	5
1973 13 SEP	4.5		4.8	10	Agua Caliente Spgs., CA	6
1975 01 AUG	5.8	5.8	5.7	14	Oroville, CA	7
1976 20 JUN	4.4		4.5	17	Susanville, CA	8
1978 04 SEP	4.7		5.0	2	Diamond Valley, CA	9
1980 27 JUL	5.2	4.7		7	Sharpsburg, KY	this paper
1981 14 FEB	10.0	4.9	5.5	5	Elk Lake, WA	5
1981 28 MAY	4.8	4.3	5.0	5	Goat Rocks, WA	11

References:

1. Eaton et al (1970)
2. Wu (1968)
3. Thatcher and Hamilton (1973)
4. Ellsworth (1975)
5. Stierman and Ellsworth (1976)
6. Allison et al (1978)
7. Morrison et al (1976)
8. Mohler (1980)
9. Somerville et al (1980)
10. Grant et al (1981)
11. Zollweg and Crosson (1981)

Figure 1. The nodal planes satisfy surface-wave spectral amplitude data as well as P-wave first motion data. Circles and triangles indicate compressional and dilatational first motion, respectively. The symbols T and P are intersections of the tension and pressure axes, respectively, with the lower hemisphere. An equal area lower hemisphere projection is used. Only sharp, impulsive first motion data are used. The northeast nodal plane strikes 30° , dips 60° and has a slip angle of 180° .

27 JUL 80

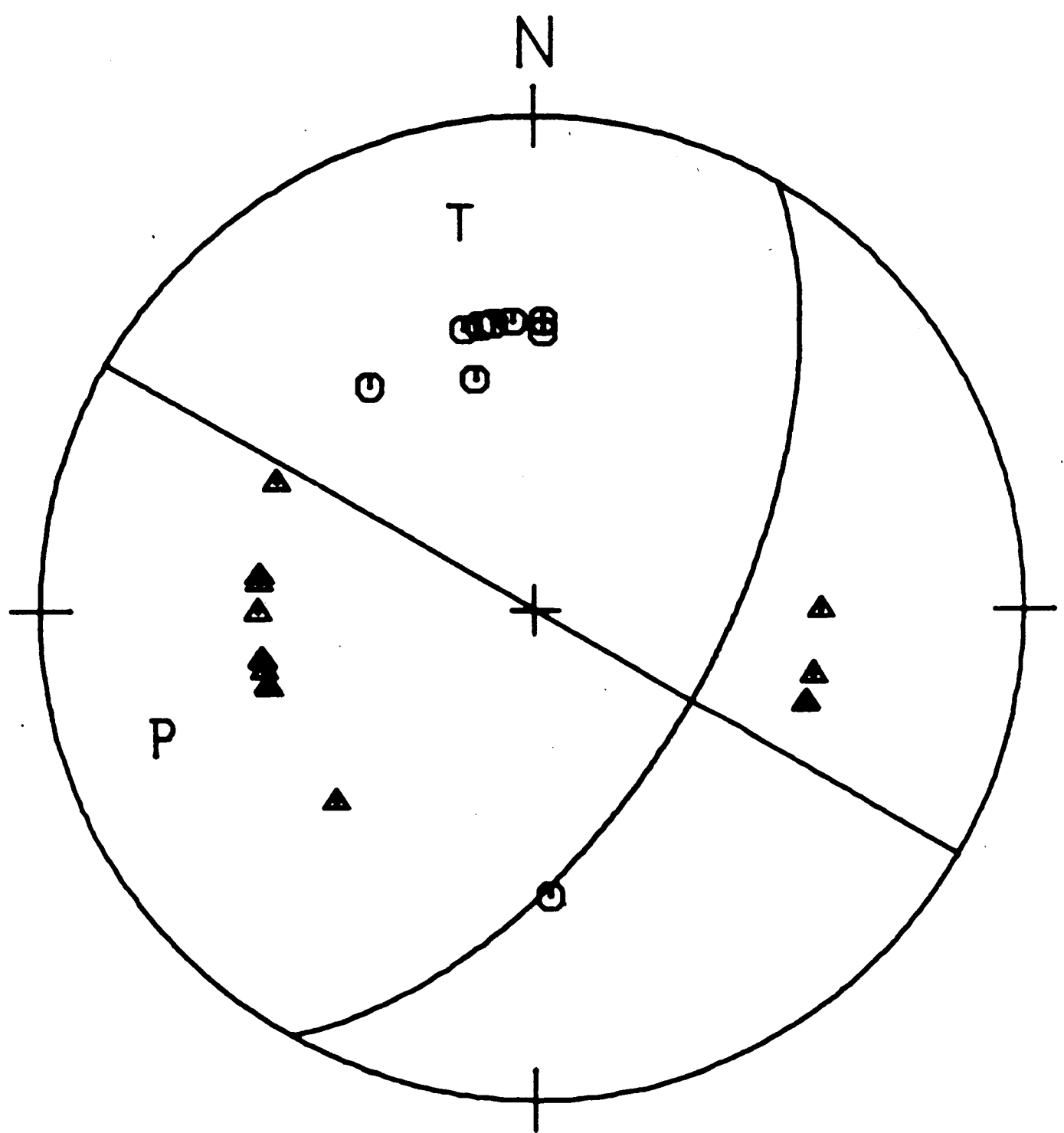
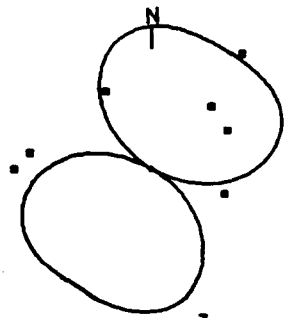


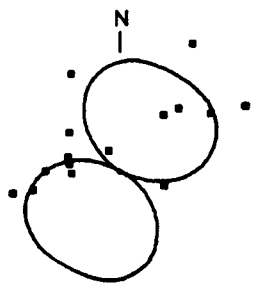
Figure 2. Comparison between anelastic attenuation corrected, observed and predicted Love-wave and Rayleigh-wave radiation patterns at selected periods T . The scaling bars are spectral amplitudes in units of cm-sec at a reference distance of 9° from the source.

SIU

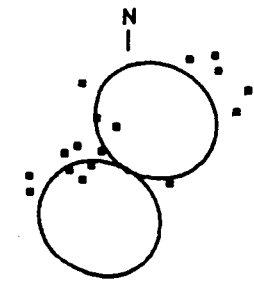
RAYLEIGH



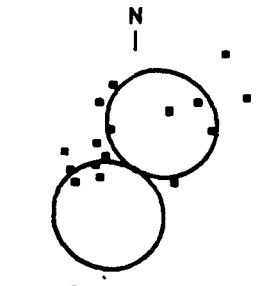
2×10^{-3}
 $T = 7.0$



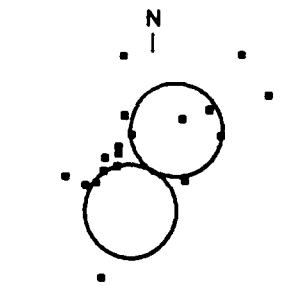
2×10^{-2}
 $T = 10.0$



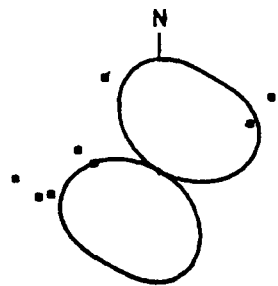
2×10^{-2}
 $T = 16.0$



2×10^{-2}
 $T = 20.0$

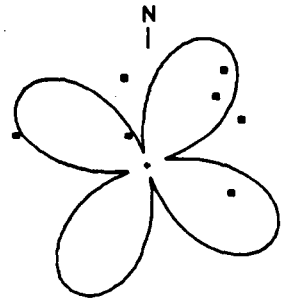


2×10^{-2}
 $T = 24.0$

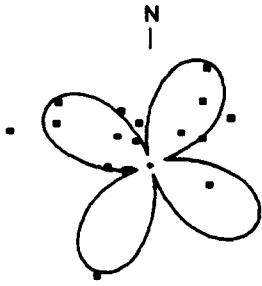


2×10^{-3}
 $T = 35.0$

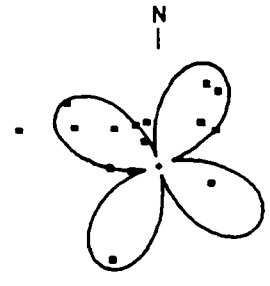
LOVE



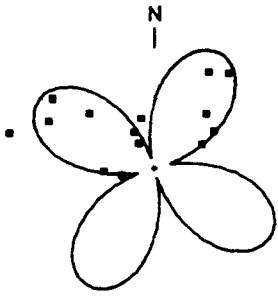
2×10^{-2}
 $T = 8.0$



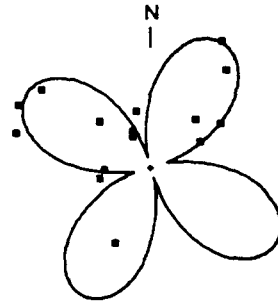
2×10^{-2}
 $T = 16.0$



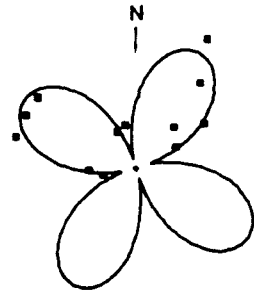
2×10^{-2}
 $T = 20.0$



2×10^{-2}
 $T = 24.0$

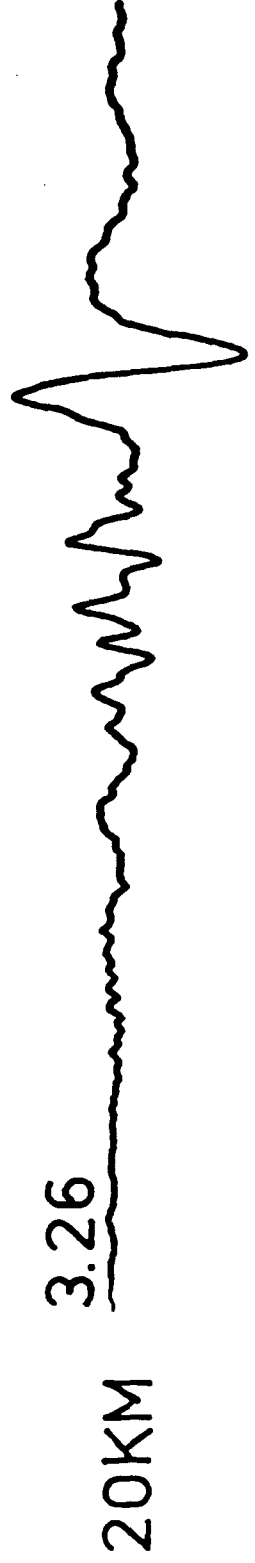
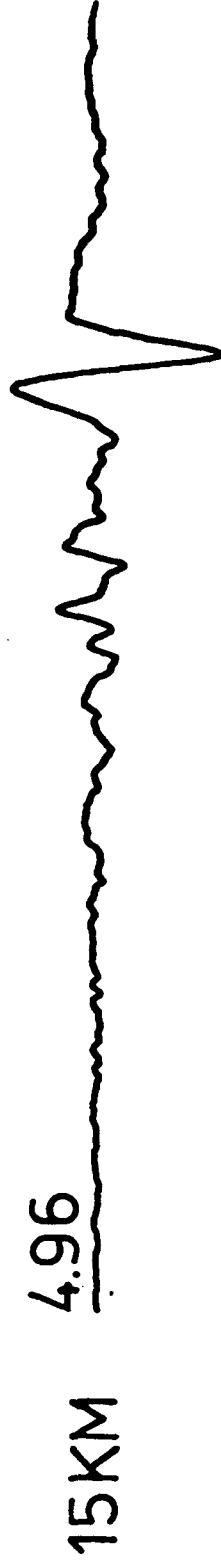
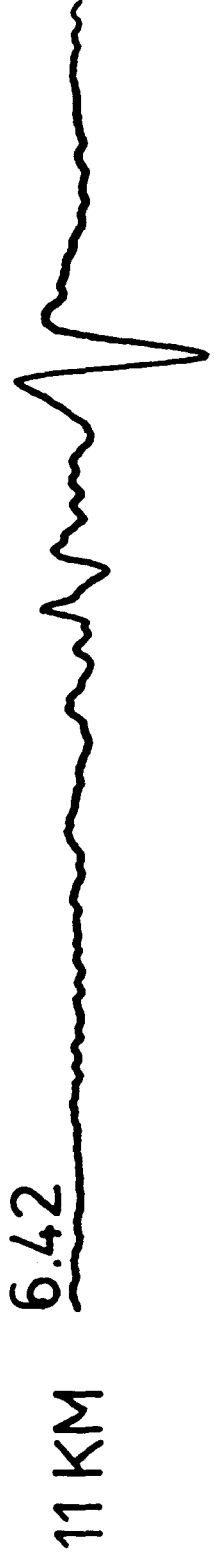
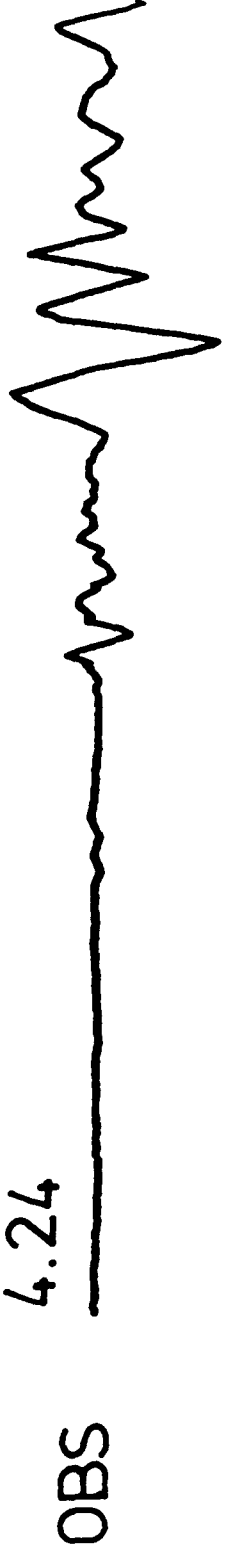


2×10^{-2}
 $T = 30.0$



2×10^{-2}
 $T = 35.0$

Figure 3. Observed and predicted long period vertical seismograms at *SLIM*, a distance of 555 km from the earthquake. 128 seconds of time history are plotted starting 90 seconds after the origin time. The number by each trace is the zero-to-peak amplitude in cm on a 15-100 WWSSN long period seismogram with peak magnification of 3000. Predicted traces are for depths of 11, 15 and 20 km in the Central U. S. earth model.



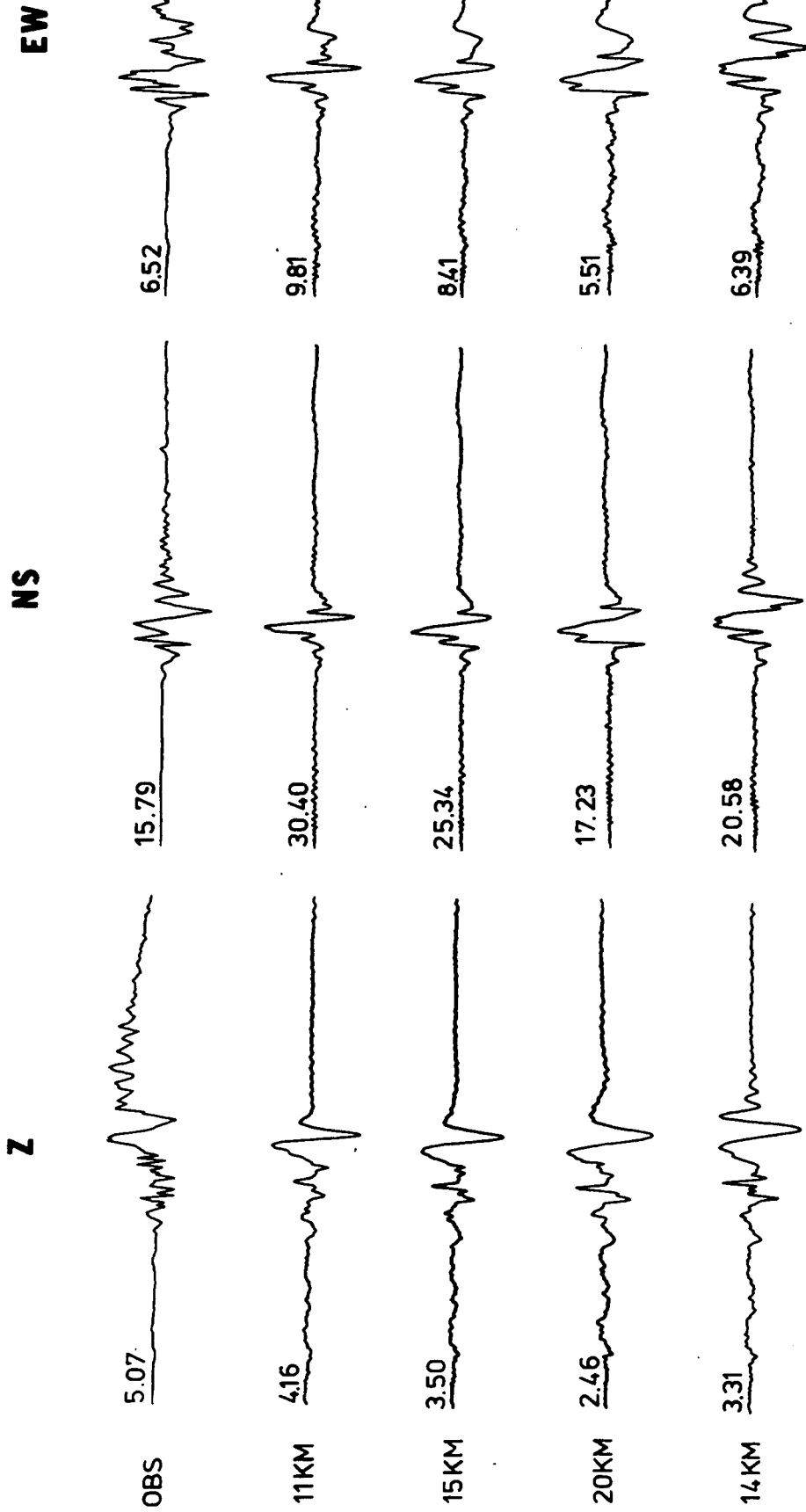


Figure 4. Observed and predicted long period three component seismograms at

BLA, a distance of 326 km from the earthquake. 128 seconds of time history are plotted, with traces starting 40.2 seconds after the origin time. The number by each trace is the zero-to-peak amplitude in cm on a 15-100 WWSSN long period seismogram with peak magnification of 3000. The central U. S. model was used for depths of 11, 15 and 20 km while the Appalachian Basin model was used for the focal depth of 14 km.

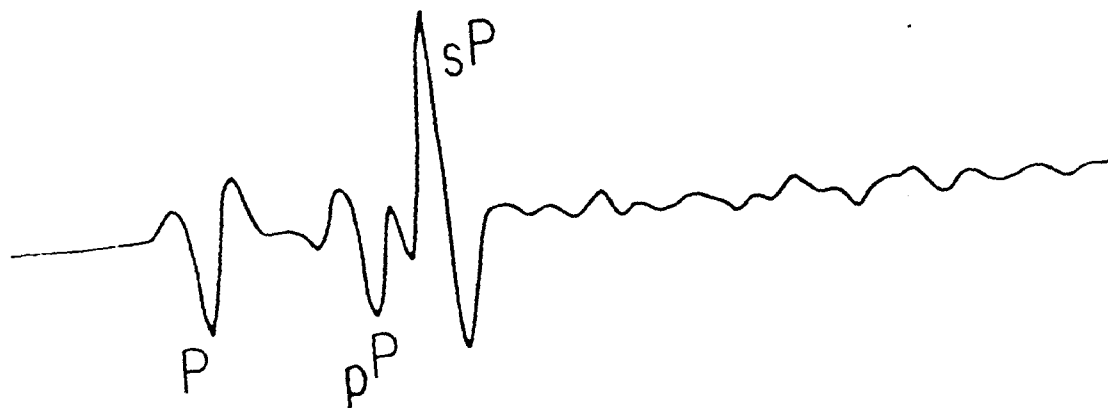
Figure 5. Observed (top) P waveform at NORSAR with synthetic waveforms (below). Crustal model, dip, strike and rake angles are given for each synthetic. Zero-to-peak amplitude for the observed trace is in quantized units (Q. U.). For NORSAR sensors, there are 0.0427 nm/ Q. U. at 1.0 Hz.

800 Q.U.

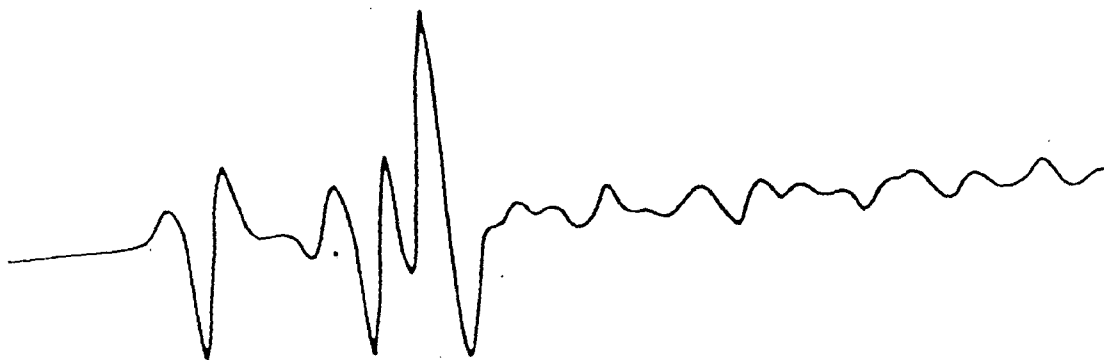
NORSAR
SUM



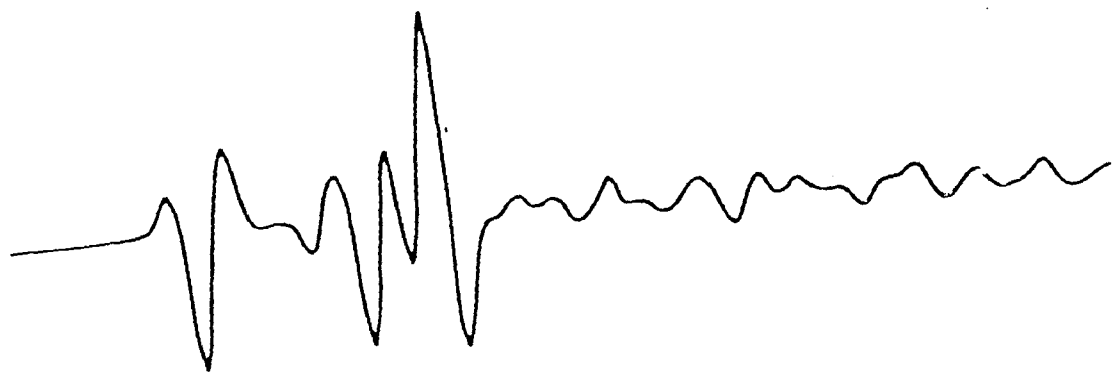
$\delta = 70^\circ$
 $s = 30^\circ$
 $\lambda = 180^\circ$
CRUST A



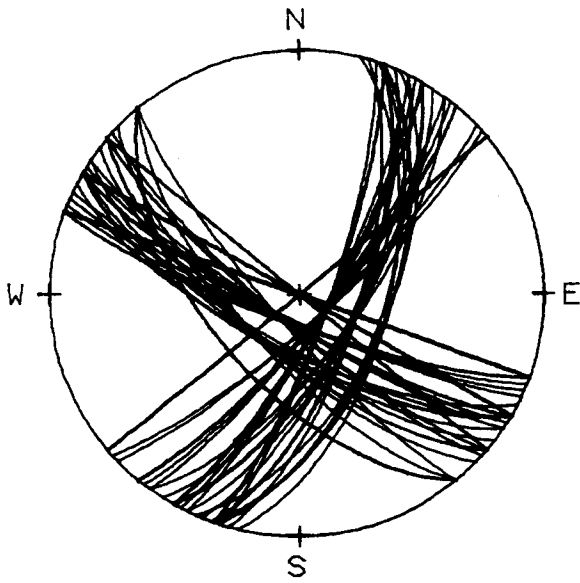
$\delta = 70^\circ$
 $s = 30^\circ$
 $\lambda = 180^\circ$
CRUST C



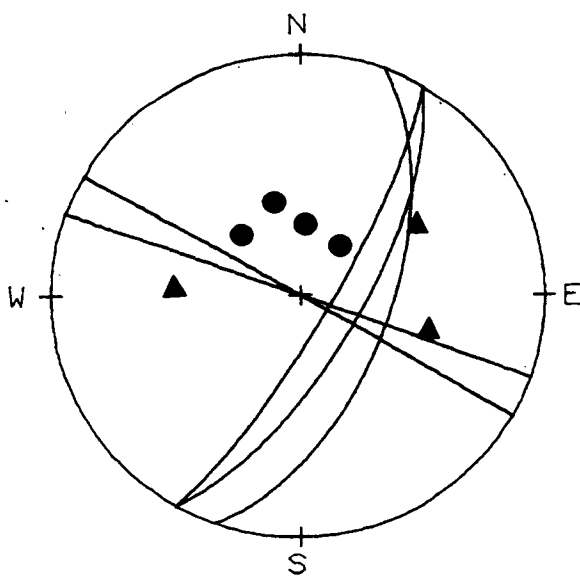
$\delta = 50^\circ$
 $s = 30^\circ$
 $\lambda = 180^\circ$
CRUST C



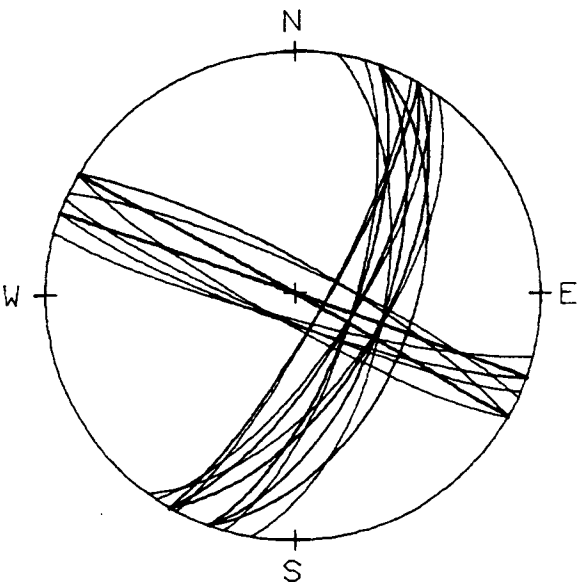
25 SEC



POLARITIES
ONLY



POLARITIES
+
NORSAR RELATIVE
AMPLITUDES
CRUST MODEL A
($\sigma = 0.5$)



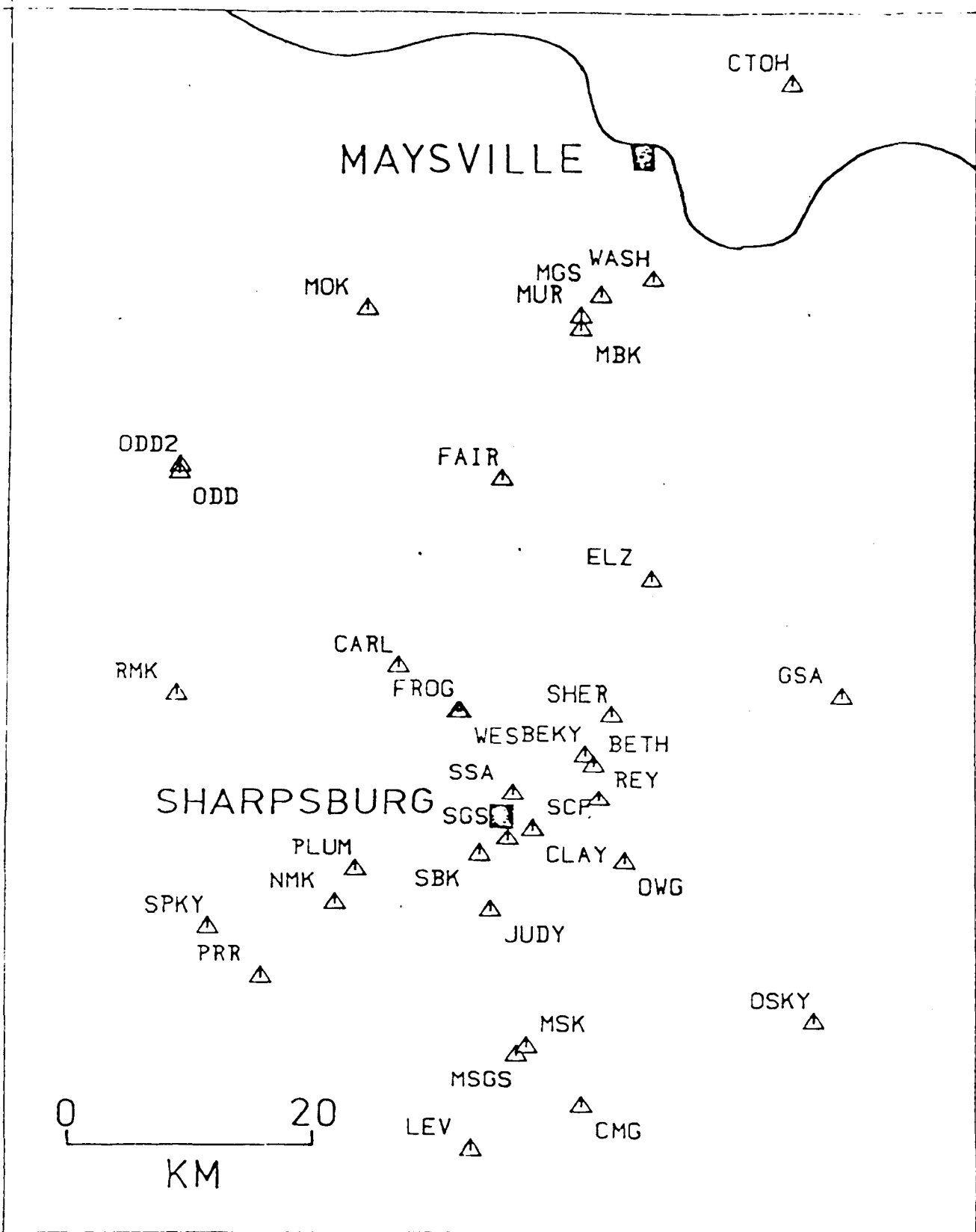
POLARITIES
+
NORSAR RELATIVE
AMPLITUDES
CRUST MODEL B
($\sigma = 0.5$)

Figure 6. Acceptable fault plane solutions for the body wave data from the Sharpsburg earthquake under various assumptions concerning the input data. P nodal planes are shown on an equal area projection of the lower focal hemisphere. All solutions are right-lateral on the NE trending planes. All possible solutions were tested with an increment angle of 5° in strike, dip, and slip.

-84.4

-83.5

38.8



0 20
KM

-84.4

-83.5

37.9

Figure 7. Locations of portable seismograph stations deployed for the aftershock study. The station coordinates are given in Table 4. The locations of Maysville and Sharpsburg, Kentucky are indicated.

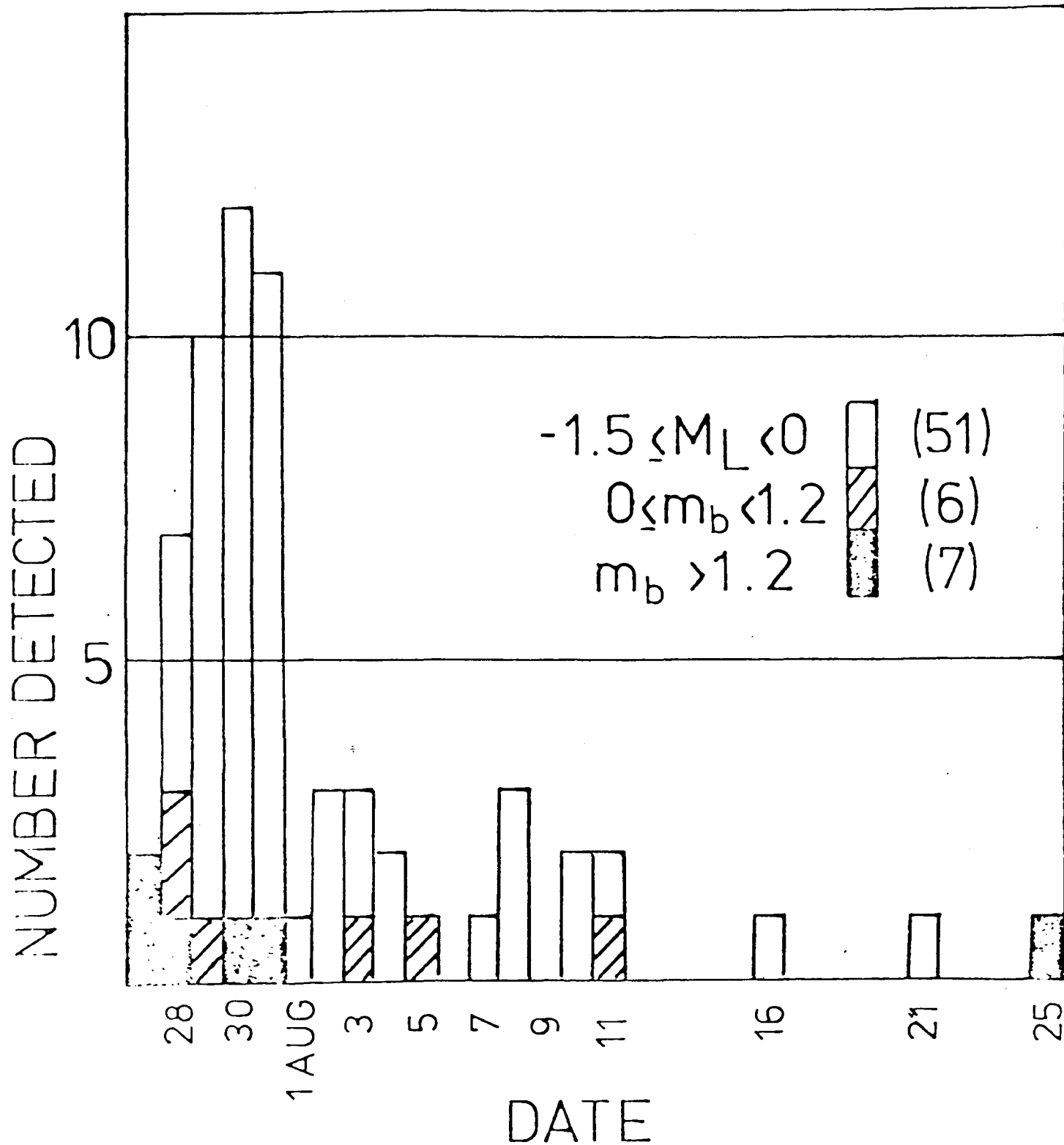
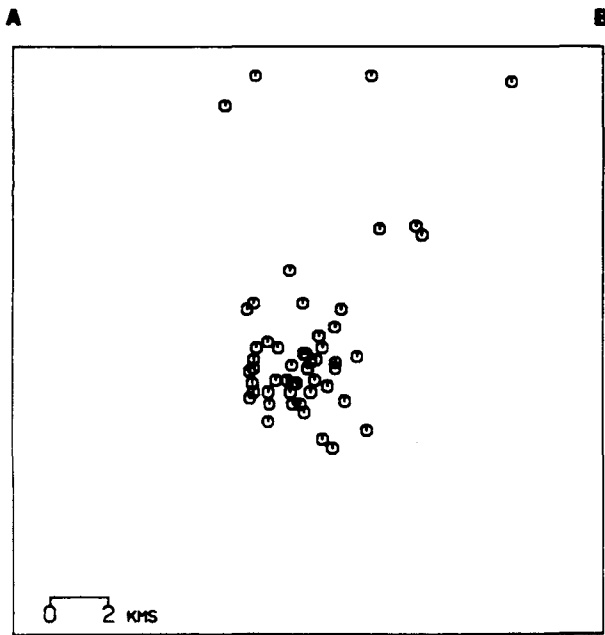
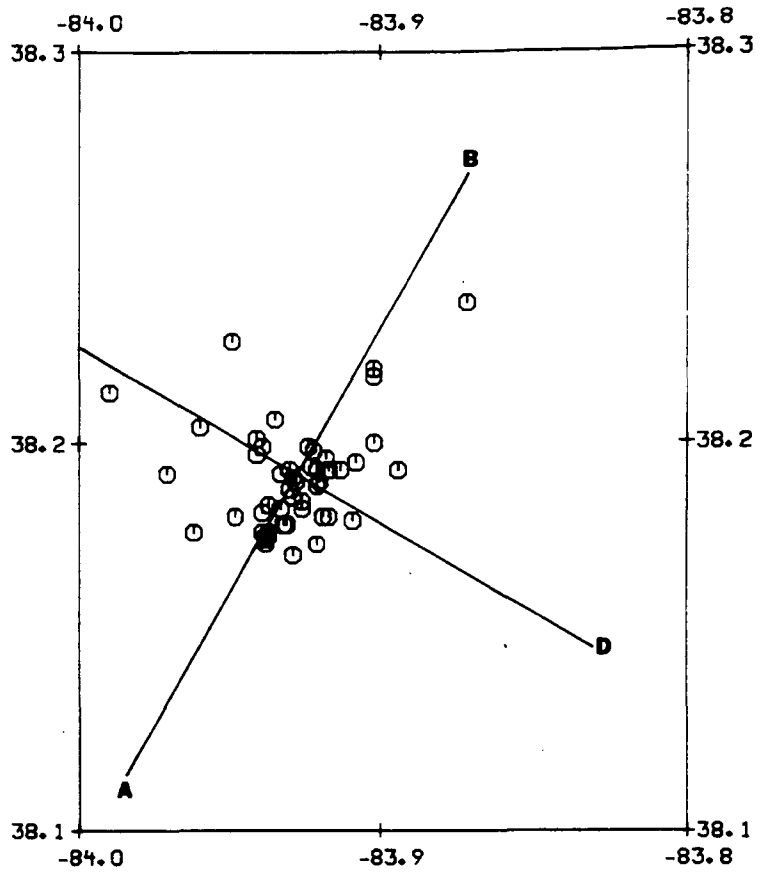
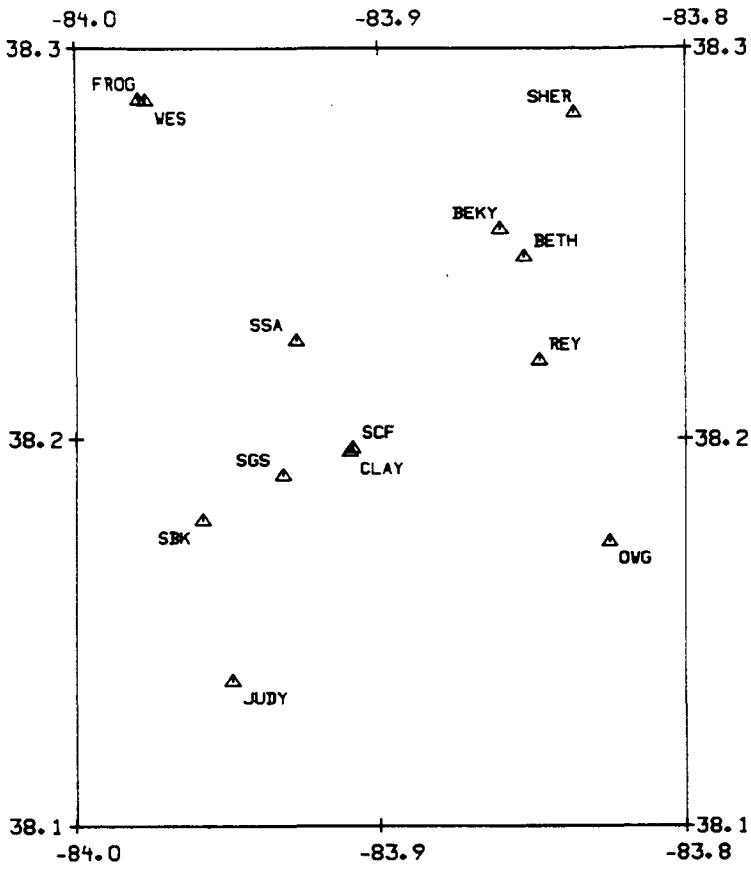
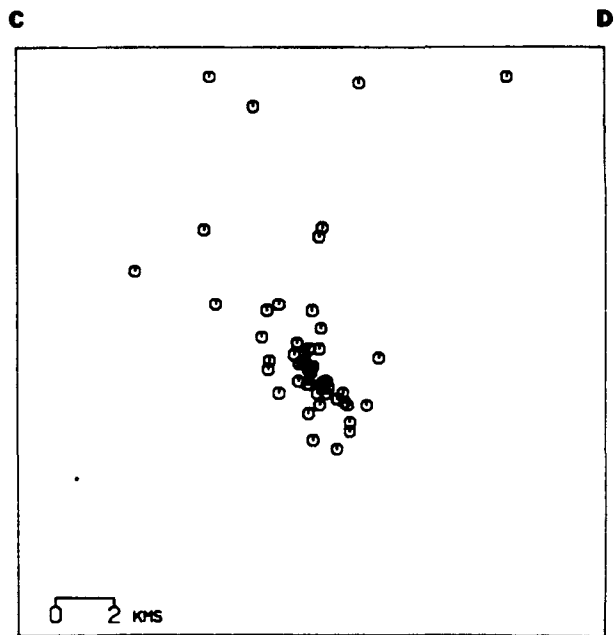


Figure 8. Plot of aftershock activity rate through August 25, 1980.



VERTICAL PROFILE CENTERED AT 38.191° N 83.928° W WITH STRIKE 30°



VERTICAL PROFILE CENTERED AT 38.191° N 83.928° W WITH STRIKE 120°

Figure 9. Hypocenter locations after using relocation techniques. Epicenters and two vertical depth profiles are shown. The seismograph stations are indicated by triangles with their names given on the base map. There is no vertical exaggeration on the depth profiles. Profile AB strikes N30°E and profile CD strikes N120°E.

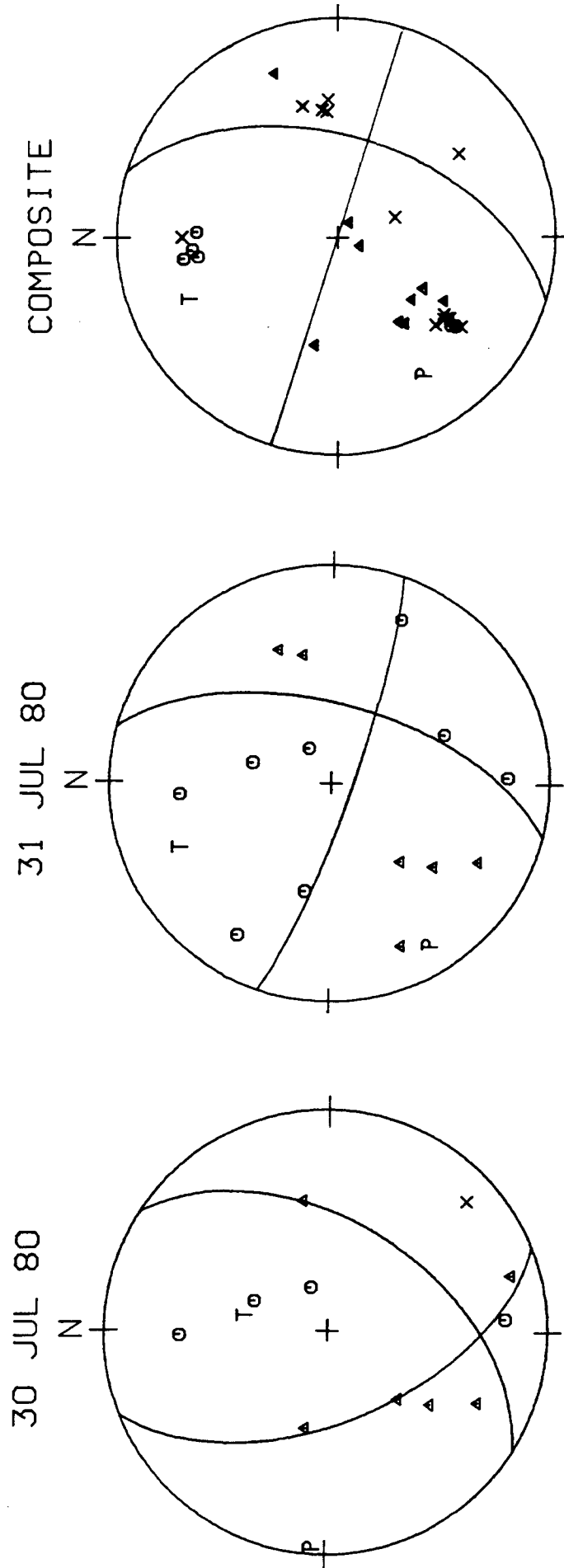


Figure 10. Lower hemisphere, equal-area projections of focal mechanism solutions for two well recorded Sharpshurg aftershocks, and a composite solution for the remaining better located aftershocks. Solid circles and triangles indicate sharp compressional and dilatational first arrivals, respectively. Open symbols denote poorer quality but clear first arrivals. Nodal quality arrivals are denoted by an X.

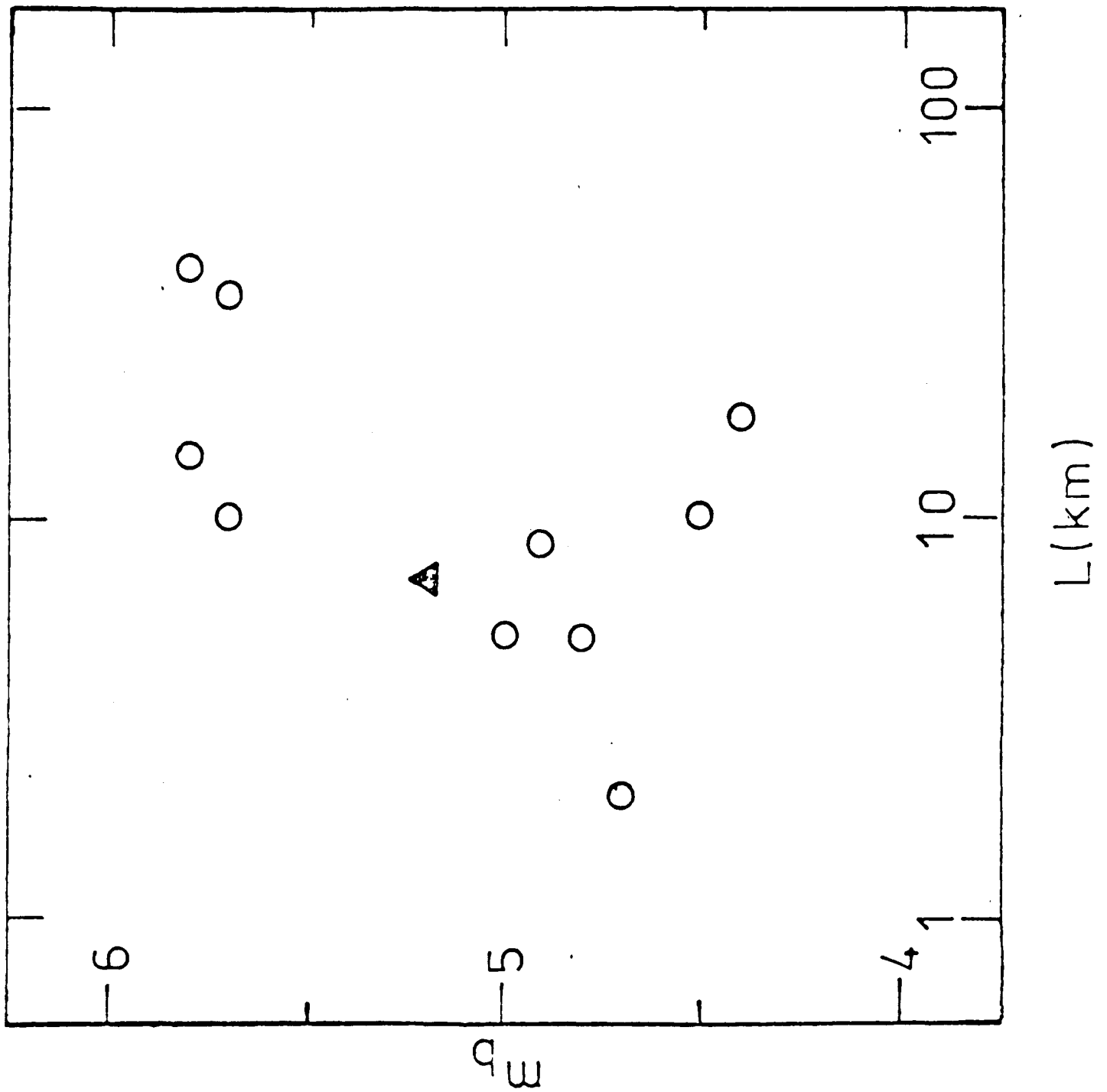


Figure 11. Plot of teleseismic m_b versus fault length for earthquakes listed in Table 7. The open symbols are western events and the solid symbol is the Sharpsburg event.